frequency where the phase reaches -2π radians (which we define as f_0), oscillations of AP and SNA will occur at around f_0. In our actual data, f_0 was approximately 0.13 Hz (Fig. 3*E*), which is consistent with a previous study (Malpas & Burgess, 2000) showing increased 0.1 Hz oscillation of AP during haemorrhage in rabbits. Moreover, the gain at f_0 was less than 1 (Fig. 3*E*), indicating no oscillations generated according to the baroreflex loop theory. Therefore, in the closed-loop-spontaneous condition, the baroreflex loop theory would not contribute to the 0.4 Hz fluctuations of AP and SNA.

Lastly, respiratory-mediated fluctuation of AP may contribute to SNA fluctuation via baroreflex mechanisms. In the baroreflex open-loop condition (Fig. 3*B*), SNA autospectrum shows no peak whereas systemic AP shows a large peak at the frequency of artificial respiration (approximately 0.57 Hz) (Fig. 3*B*). This indicates that AP fluctuation at that frequency is not mediated by SNA but by mechanical aspects of respiration (i.e. respiratory changes in intrathoracic pressure), consistent with an earlier report (Brychta *et al.* 2007). Since closing the baroreflex loop produces a peak in the SNA autospectrum at the respiratory frequency (Fig. 4*B*), a baroreflex mechanism may partly be responsible for respiratory-mediated SNA fluctuation in this experimental condition.

Physiological implication (3): open-loop baroreflex neural arc transfer function is able to predict closed-loop time-series SNA response to drug-induced AP change

The data discussed so far were obtained using mechanical interventions to change carotid sinus pressure, which arguably are not physiological changes. To validate whether the predictabilities of the open-loop and closed-loop-spontaneous transfer functions apply to more physiological conditions, we tested the neural arc transfer functions using pharmacological pressure intervention (phenylephrine and nitroprusside infusions) under closed-loop conditions. First, the SNA predicted by the open-loop baroreflex neural arc transfer function ($H_{\text{n-open}}$) in response to the measured changes in CSP (= AP) was roughly similar to the actually measured SNA with respect to both amplitude and timing of neural activity (Fig. 10*A*, third and fourth panel), showing high correlation ($r^2 = 0.9$, Fig. 10*B*). This result indicates that with regard to the neural arc, the open-loop transfer function is able to predict time-series SNA output from AP input even during pharmacological pressure interventions. A possible explanation for the good predictability is that since the pharmacological interventions exert a noise to the peripheral and not the neural arc, time-series SNA is almost determined by the pharmacologically induced changes in baroreceptor pressure (= systemic AP) via the neural arc transfer function (= $H_{\text{n-open}}$).

In contrast to the open-loop transfer function, the SNA predicted by the closed-loop-spontaneous baroreflex neural arc transfer function ($H_{\text{n-closed-spon}}$) was different from the measured SNA. The predicted SNA was an oppositely directed neural response: when AP (= CSP) increased, the predicted SNA increased whereas the measured SNA decreased, and vice versa. Therefore, with regard to the neural arc, the closed-loop-spontaneous transfer function is not able to predict SNA dynamics from AP. The failure in predicting SNA change may be explained by inappropriate system identification in the closed-loop condition. Because of the closed-loop condition, the calculated phase function of $H_{\text{n-closed-spon}}$ was the inverse of that of $H_{\text{p-closed-spon}}$. Indeed, the phase led as frequency increased (Figs 5, 11*B* and *D*) in contrast to the phase lag of the open-loop transfer function ($H_{\text{n-open}}$). Furthermore, the calculated phase of $H_{\text{n-closed-spon}}$ resulted in an oppositely directed response of predicted SNA as compared with actually measured SNA, in contrast to the good match of predicted SNA by $H_{\text{n-open}}$. These results indicate that with regard to the neural arc, the open-loop neural arc transfer function predicts time-series SNA response to changes in AP induced by pharmacological interventions, while the closed-loop-spontaneous transfer function cannot predict SNA response.

Although spontaneous baroreflex measures are believed to represent the neural arc function (baroreflex control of SNA), the present study raises potential methodological issues. First, since the baroreflex is a closed-loop feedback system, there is theoretical difficulty in identifying system characteristics in the closed-loop spontaneous condition. Since a relationship calculated from SNA input to AP during their spontaneous fluctuations is the inverse of that calculated from AP input to SNA, the calculation itself cannot determine the causality between them. Our present data clearly indicate limitation in estimating closed-loop-spontaneous transfer function of the neural arc, and that a good estimation requires opening the loop and introducing an intervention to the loop. Furthermore, although the spontaneous baroreflex transfer function obtained in the closed-loop condition (Orea *et al.* 2007; Cooke *et al.* 2009; Ogoh *et al.* 2009) has been used as a surrogate for the neural (feedback) arc function of the baroreflex loop, it actually represents the peripheral (feedforward) arc function since baroreflex loop is predominantly feedforward rather than feedback in the closed-loop-spontaneous condition.

Second, a recent study (Hart *et al.* 2010) has reported that spontaneous baroreflex measures (slope of strength of muscle SNA burst over-binned or non-binned AP) did not correlate ($r^2 = 0.05$–0.13) with the 'gold standard' modified Oxford analysis (nitroprusside and phenylephrine), whereas spontaneous threshold measure

(slope of % occurrence of muscle SNA burst over 1 mmHg binned AP, eliminating strength of SNA burst) correlated with it mildly ($r^2 = 0.5$). Although we cannot directly compare the transfer function analysis in our present study with the spontaneous threshold measure reported by Hart *et al.* (2010) because of methodological differences, our open-loop transfer function of the neural arc was able to predict occurrence and magnitude of time-series SNA with a higher degree of accuracy ($r^2 = 0.9$, Fig. 10*B*) and reproduce the AP–SNA relationship during closed-loop, drug-induced AP changes (Fig. 10*D*).

Limitations

The present study has several limitations. First, we excluded the efferent effect of the vagally mediated arterial baroreflex, which could affect the properties of baroreflex control of SNAs. Second, artificial respiration and surgical procedures used in this study could affect baroreflex. Third, anaesthetic agents tend to inhibit efferent SNA and depress the gain of baroreflex control of SNA. Fourth, since the present study was animal research, it is limited in its applicability to humans. However, a problem of difficulty in identifying the 'closed-loop' system in contrast with the 'open-loop' system is common in animal and human studies. Lastly, we perfused the carotid sinuses with physiological saline pre-equilibrated with atmospheric. Local hypoxia could have occurred and somewhat affected baroreflex control of SNA. Further research to examine the relevance of the present findings to true physiological conditions is necessary.

Summary

In summary, the open-loop baroreflex transfer functions for the neural and peripheral arcs allowed good prediction of the time-series SNA and AP outputs from baroreceptor pressure and SNA inputs, respectively. In contrast, the closed-loop-spontaneous baroreflex transfer function for the neural arc deviated greatly from the open-loop transfer function, and could not predict the time-series SNA dynamics. However, the closed-loop-spontaneous baroreflex transfer function for the peripheral arc partially matched the open-loop transfer function, with reasonable predictability of the time-series AP dynamics although slightly inferior in accuracy. Furthermore, the predictabilities of open-loop and closed-loop-spontaneous transfer functions of the neural arc were validated by closed-loop pharmacological (phenylephrine and nitroprusside infusions) pressure interventions. Time-series SNA responses to drug-induced AP changes predicted by the open-loop transfer function matched closely the measured responses, whereas SNA responses predicted by the closed-loop-spontaneous transfer function deviated greatly and were the inverse of measured responses. Therefore, although the spontaneous baroreflex transfer function obtained by closed-loop analysis has been believed to represent the neural arc function, it is inappropriate for system identification of the neural arc but is partially appropriate for system identification of the peripheral arc under resting condition, compared with open-loop analysis.

Appendix A

In a block diagram of the open-loop baroreflex system (Fig. 1*A*), CSP is independent of systemic AP because of vascular isolation of the carotid-sinus regions. In this framework, input–output relationships of these arcs are expressed in the frequency domain as:

$$\mathrm{SNA}(f) = H_\mathrm{n}(f) \cdot \mathrm{CSP}(f) + \mathrm{NN}(f) \qquad \text{(A1)}$$

$$\mathrm{AP}(f) = H_\mathrm{p}(f) \cdot \mathrm{SNA}(f) + \mathrm{PN}(f) \qquad \text{(A2)}$$

where CSP(f), SNA(f) and AP(f) are the fast Fourier transforms of CSP, SNA and systemic AP, respectively. $H_\mathrm{n}(f)$ and $H_\mathrm{p}(f)$ denote the neural arc and the peripheral arc transfer functions, respectively. NN(f) and PN(f) represent unknown noise in the neural and peripheral arcs, respectively.

In the neural arc, calculating the ensemble averages of cross-powers between the terms of eqn (A1) and CSP(f) yields

$$E[\mathrm{SNA}(f) \cdot \mathrm{CSP}(f)^*] = H_\mathrm{n}(f) \cdot E[\mathrm{CSP}(f) \cdot \mathrm{CSP}(f)^*] + E[\mathrm{NN}(f) \cdot \mathrm{CSP}(f)^*] \qquad \text{(A3)}$$

where $E[]$ indicates an ensemble average operation. CSP(f)* denotes the complex conjugate of CSP(f). As $H_\mathrm{n}(f)$ is supposed to be time invariant during the observation period, $H_\mathrm{n}(f)$ is outside the ensemble average operation. When CSP is a white-noise signal, E[NN(f)·CSP(f)*] diminishes to zero asymptotically because the white noise is statistically independent of any other noise signal. Thus, we can estimate $H_\mathrm{n}(f)$ by the following equation, which we designate $H_\mathrm{n\text{-}open}(f)$.

$$H_\mathrm{n}(f) = \frac{E[\mathrm{SNA}(f) \cdot \mathrm{CSP}(f)^*]}{E[\mathrm{CSP}(f) \cdot \mathrm{CSP}(f)^*]} = H_\mathrm{n\text{-}open}(f) \qquad \text{(A4)}$$

Similarly, in the peripheral arc, calculating ensemble averages of cross-powers between terms of eqn (A2) and SNA(f) yields

$$E[\mathrm{AP}(f) \cdot \mathrm{SNA}(f)^*] = H_\mathrm{p}(f) \cdot E[\mathrm{SNA}(f) \cdot \mathrm{SNA}(f)^*] + E[\mathrm{PN}(f) \cdot \mathrm{SNA}(f)^*] \qquad \text{(A5)}$$

where SNA(f)* denotes the complex conjugate of SNA(f). As $H_\mathrm{p}(f)$ is supposed to be time invariant during the

observation period, $H_p(f)$ is outside the ensemble average operation. In the open-loop condition, since PN(f) cannot affect SNA(f) and is statistically independent of SNA(f) by definition, E[PN(f)·SNA(f)*] diminishes to zero asymptotically. Thus, we can estimate $H_p(f)$ by the following equation, which we designate $H_{p\text{-open}}(f)$.

$$H_p(f) = \frac{E[\mathrm{AP}(f)\cdot\mathrm{SNA}(f)^*]}{E[\mathrm{SNA}(f)\cdot\mathrm{SNA}(f)^*]} = H_{p\text{-open}}(f) \quad \text{(A6)}$$

In contrast to the open-loop condition, CSP is matched with systemic AP in the closed-loop-spontaneous baroreflex condition (Fig. 1*B*). Thus, the input–output relationships of the arcs in the frequency domain are expressed as:

$$\mathrm{SNA}(f) = H_n(f)\cdot\mathrm{AP}(f) + \mathrm{NN}(f) \quad \text{(A7)}$$

$$\mathrm{AP}(f) = H_p(f)\cdot\mathrm{SNA}(f) + \mathrm{PN}(f) \quad \text{(A8)}$$

In the neural arc, calculating ensemble averages of cross-powers between the terms of eqn (A7) and AP(f) yields

$$E[\mathrm{SNA}(f)\cdot\mathrm{AP}(f)^*] = H_n(f)\cdot E[\mathrm{AP}(f)\cdot\mathrm{AP}(f)^*] + E[\mathrm{NN}(f)\cdot\mathrm{AP}(f)^*] \quad \text{(A9)}$$

$$H_n(f) = \frac{E[\mathrm{SNA}(f)\cdot\mathrm{AP}(f)^*]}{E[\mathrm{AP}(f)\cdot\mathrm{AP}(f)^*]} - \frac{E[\mathrm{NN}(f)\cdot\mathrm{AP}(f)^*]}{E[\mathrm{AP}(f)\cdot\mathrm{AP}(f)^*]} \quad \text{(A10)}$$

However, in the baroreflex closed-loop conditions, the unknown noise in SNA (NN) can affect AP through the peripheral arc transfer function (H_p). In other words, AP(f) inevitably correlates with NN(f), and E[NN(f)·AP(f)*] does not diminish to zero. $H_n(f)$ cannot be determined because the unknown noise NN is practically impossible to quantify. Therefore in protocol 3, we simplify eqn (A10) by neglecting the last term, and define the closed-loop-spontaneous transfer function by the following equation, which we designate $H_{n\text{-closed-spon}}(f)$.

$$H_n(f) = \frac{E[\mathrm{SNA}(f)\cdot\mathrm{AP}(f)^*]}{E[\mathrm{AP}(f)\cdot\mathrm{AP}(f)^*]} = H_{n\text{-closed-spon}}(f) \quad \text{(A11)}$$

However, from eqns (A4) and (A11), it is evident that $H_{n\text{-closed-spon}}(f)$ should be different from $H_{n\text{-open}}(f)$ when NN(f) is large and cannot be neglected.

In the peripheral arc, calculating ensemble averages of cross-powers between the terms of eqn (A8) and SNA(f) yields:

$$E[\mathrm{AP}(f)\cdot\mathrm{SNA}(f)^*] = H_p(f)\cdot E[\mathrm{SNA}(f)\cdot\mathrm{SNA}(f)^*] + E[\mathrm{PN}(f)\cdot\mathrm{SNA}(f)^*] \quad \text{(A12)}$$

$$H_p(f) = \frac{E[\mathrm{AP}(f)\cdot\mathrm{SNA}(f)^*]}{E[\mathrm{SNA}(f)\cdot\mathrm{SNA}(f)^*]} - \frac{E[\mathrm{PN}(f)\cdot\mathrm{SNA}(f)^*]}{E[\mathrm{SNA}(f)\cdot\mathrm{SNA}(f)^*]} \quad \text{(A13)}$$

However, in the baroreflex closed-loop conditions, the unknown noise in AP (PN) can affect SNA through the neural arc transfer function (H_n). In other words, SNA(f) inevitably correlates with PN(f), and E[PN(f)·SNA(f)*] does not diminish to zero. $H_p(f)$ cannot be determined because the unknown noise PN is practically impossible to quantify. Therefore in protocol 3, we simplify eqn (A13) by neglecting the last term and define the closed-loop-spontaneous transfer function by the following equation, which we designate $H_{p\text{-closed-spon}}(f)$.

$$H_p(f) = \frac{E[\mathrm{AP}(f)\cdot\mathrm{SNA}(f)^*]}{E[\mathrm{SNA}(f)\cdot\mathrm{SNA}(f)^*]} = H_{p\text{-closed-spon}}(f) \quad \text{(A14)}$$

However, from eqns (A6) and (A14), it is evident that $H_{p\text{-closed-spon}}(f)$ should be different from $H_{p\text{-open}}(f)$ when PN(f) is large and cannot be neglected.

Appendix B

In rabbits, the transfer function of the baroreflex neural arc (baroreceptor pressure/CSP to SNA) approximates derivative characteristics in the frequency range below 0.8 Hz, and high-cut characteristics of frequencies above 0.8 Hz (Kawada *et al.* 2002). Therefore, according to our previous study, we model the neural arc transfer function (H_n) using eqn (B1) as follows

$$H_n(f) = -K_n \frac{1+\frac{f}{f_{c1}}j}{\left(1+\frac{f}{f_{c2}}\right)^2}\exp(-2\pi f j L) \quad \text{(B1)}$$

where f and j represent the frequency (in Hz) and imaginary units, respectively; K_n is static gain (in a.u. mmHg^{-1}); f_{c1} and f_{c2} ($f_{c1} < f_{c2}$) are corner frequencies (in Hz) for derivative and high-cut characteristics, respectively; and L is a pure delay (in s), that would represent the sum of delays in synaptic transmission in the baroreflex central pathways and the sympathetic ganglion. The dynamic gain increases in the frequency range from f_{c1} to f_{c2}, and decreases above f_{c2}. Based on the measured results, we set K_n, f_{c1}, f_{c2} and L at 1, 0.1, 0.8 and 0.2, respectively, in all simulations in Fig. 11.

In addition, the transfer function of the baroreflex peripheral arc (SNA to systemic AP) approximates the second-order low-pass filter with a lag time in rabbits (Kawada *et al.* 2002). Therefore, we model the peripheral

arc transfer function (H_p) using eqn (B2) as follows:

$$H_p(f) = \frac{K_p}{1 + 2\zeta\frac{f}{f_N}j + \left(\frac{f}{f_N}j\right)^2} \exp(-2\pi f j L) \quad \text{(B2)}$$

where K_p is static gain (in mmHg a.u.$^{-1}$); fN and ζ indicate a natural frequency (in Hz) and a damping ratio, respectively; and L is a pure delay (in s) that would represent the sum of delays in synaptic transmission in the neuroeffector junction and intracellular signal transduction in the effector organs. Based on the measured results, we set K_p, f_N, ζ and L at 1, 0.07, 1.4 and 1.0, respectively, in all simulations in Fig. 11.

References

Barres C, Cheng Y & Julien C (2004). Steady-state and dynamic responses of renal sympathetic nerve activity to air-jet stress in sinoaortic denervated rats. *Hypertension* **43**, 629–635.

Brychta RJ, Shiavi R, Robertson D, Biaggioni I & Diedrich A (2007). A simplified two-component model of blood pressure fluctuation. *Am J Physiol Heart Circ Physiol* **292**, H1193–H1203.

Cooke WH, Hoag JB, Crossman AA, Kuusela TA, Tahvanainen KU & Eckberg DL (1999). Human responses to upright tilt: a window on central autonomic integration. *J Physiol* **517**, 617–628.

Cooke WH, Rickards CA, Ryan KL, Kuusela TA & Convertino VA (2009). Muscle sympathetic nerve activity during intense lower body negative pressure to presyncope in humans. *J Physiol* **587**, 4987–4999.

deBoer RW, Karemaker JM & Strackee J (1987). Hemodynamic fluctuations and baroreflex sensitivity in humans: a beat-to-beat model. *Am J Physiol Heart Circ Physiol* **253**, H680–H689.

DiBona GF & Sawin LL (2003). Frequency response of the renal vasculature in congestive heart failure. *Circulation* **107**, 2159–2164.

DiBona GF & Sawin LL (2004). Effect of renal denervation on dynamic autoregulation of renal blood flow. *Am J Physiol Renal Physiol* **286**, F1209–F1218.

Drummond GB (2009). Reporting ethical matters in *The Journal of Physiology*: standards and advice. *J Physiol* **587**, 713–719.

Eckberg DL & Sleight P (1992). *Human Baroreflexes in Health and Disease*. Oxford University Press, New York.

Guyton A & Harris J (1951). Pressoreceptor-autonomic oscillation: a probable cause of vasomotor waves. *Am J Physiol* **165**, 158–166.

Hart EC, Joyner MJ, Wallin BG, Karlsson T, Curry TB & Charkoudian N (2010). Baroreflex control of muscle sympathetic nerve activity: a nonpharmacological measure of baroreflex sensitivity. *Am J Physiol Heart Circ Physiol* **298**, H816–H822.

Ikeda Y, Kawada T, Sugimachi M, Kawaguchi O, Shishido T, Sato T *et al.* (1996). Neural arc of baroreflex optimizes dynamic pressure regulation in achieving both stability and quickness. *Am J Physiol Heart Circ Physiol* **271**, H882–H890.

Ikeda Y, Sugimachi M, Yamasaki T, Kawaguchi O, Shishido T, Kawada T *et al.* (1995). Explorations into development of a neurally regulated cardiac pacemaker. *Am J Physiol Heart Circ Physiol* **269**, H2141–H2146.

Julius SB & Allan GP (ed.) (2000). *Random Data: Analysis and Measurement Procedures*. John Wiley & Sons, Inc., New York.

Kamiya A, Hayano J, Kawada T, Michikami D, Yamamoto K, Ariumi H *et al.* (2005*a*). Low-frequency oscillation of sympathetic nerve activity decreases during development of tilt-induced syncope preceding sympathetic withdrawal and bradycardia. *Am J Physiol Heart Circ Physiol* **289**, H1758–H1769.

Kamiya A, Kawada T, Mizuno M, Shimizu S & Sugimachi M (2010). Parallel resetting of arterial baroreflex control of renal and cardiac sympathetic nerve activities during upright tilt in rabbits. *Am J Physiol Heart Circ Physiol* **298**, H1966–H1975.

Kamiya A, Kawada T, Yamamoto K, Michikami D, Ariumi H, Miyamoto T *et al.* (2005*b*). Dynamic and static baroreflex control of muscle sympathetic nerve activity (SNA) parallels that of renal and cardiac SNA during physiological change in pressure. *Am J Physiol Heart Circ Physiol* **289**, H2641–H2648.

Kamiya A, Kawada T, Yamamoto K, Mizuno M, Shimizu S & Sugimachi M (2008*a*). Upright tilt resets dynamic transfer function of baroreflex neural arc to minify the pressure disturbance in total baroreflex control. *J Physiol Sci* **58**, 189–198.

Kamiya A, Michikami D, Iwase S & Mano T (2008*b*). Decoding rule from vasoconstrictor skin sympathetic nerve activity to nonglabrous skin blood flow in humans at normothermic rest. *Neurosci Lett* **439**, 13–17.

Kawada T, Li M, Kamiya A, Shimizu S, Uemura K, Yamamoto H & Sugimachi M (2010). Open-loop dynamic and static characteristics of the carotid sinus baroreflex in rats with chronic heart failure after myocardial infarction. *J Physiol Sci* **60**, 283–298.

Kawada T, Zheng C, Yanagiya Y, Uemura K, Miyamoto T, Inagaki M *et al.* (2002). High-cut characteristics of the baroreflex neural arc preserve baroreflex gain against pulsatile pressure. *Am J Physiol Heart Circ Physiol* **282**, H1149–H1156.

Malpas SC & Burgess DE (2000). Renal SNA as the primary mediator of slow oscillations in blood pressure during hemorrhage. *Am J Physiol Heart Circ Physiol* **279**, H1299–H1306.

Ogoh S, Fisher JP, Young CN, Raven PB & Fadel PJ (2009). Transfer function characteristics of the neural and peripheral arterial baroreflex arcs at rest and during postexercise muscle ischemia in humans. *Am J Physiol Heart Circ Physiol* **296**, H1416–H1424.

Orea V, Kanbar R, Chapuis B, Barres C & Julien C (2007). Transfer function analysis between arterial pressure and renal sympathetic nerve activity at cardiac pacing frequencies in the rat. *J Appl Physiol* **102**, 1034–1040.

Rowell LB (1993). *Human Cardiovascular Control*. Oxford University Press, New York.

Zhang R, Zuckerman JH, Iwasaki K, Wilson TE, Crandall CG & Levine BD (2002). Autonomic neural control of dynamic cerebral autoregulation in humans. *Circulation* **106**, 1814–1820.

Author contributions

The experiments were performed at the Department of Cardiovascular Dynamics, National Cerebral and Cardiovascular Center Research Institute. A.K. absolutely contributed to: (1) Conception and design, (2) Collection, analysis and interpretation of data and (3) Drafting the article or revising it critically for important intellectual content. Other authors helped him particularly in (3). All authors approved the final version.

Acknowledgments

This study was supported by a research project promoted by Ministry of Health, Labour and Welfare in Japan (no. H21-nano-ippan-005, H22-nanchi-ippan-142), the Grants-in-Aid for Scientific Research promoted by Ministry of Education, Culture, Sports, Science and Technology in Japan (no. 20390462, 22791559) and the Industrial Technology Research Grant Program from New Energy and Industrial Technology Development Organization (NEDO) of Japan.

Am J Physiol Regul Integr Comp Physiol 300: R969–R977, 2011.
First published January 26, 2011; doi:10.1152/ajpregu.00768.2010.

Exercise training augments the dynamic heart rate response to vagal but not sympathetic stimulation in rats

Masaki Mizuno,[1,2] Toru Kawada,[2] Atsunori Kamiya,[2] Tadayoshi Miyamoto,[2,3] Shuji Shimizu,[2] Toshiaki Shishido,[2] Scott A. Smith,[1] and Masaru Sugimachi[2]

[1]*Departments of Physical Therapy and Internal Medicine, University of Texas Southwestern Medical Center at Dallas, Dallas, Texas;* [2]*Department of Cardiovascular Dynamics, National Cerebral and Cardiovascular Center Research Institute, Osaka, Japan; and* [3]*Department of Physical Therapy, Morinomiya University of Medical Sciences, Osaka, Japan*

Submitted 23 November 2010; accepted in final form 26 January 2011

Mizuno M, Kawada T, Kamiya A, Miyamoto T, Shimizu S, Shishido T, Smith SA, Sugimachi M. Exercise training augments the dynamic heart rate response to vagal but not sympathetic stimulation in rats. *Am J Physiol Regul Integr Comp Physiol* 300: R969–R977, 2011. First published January 26, 2011; doi:10.1152/ajpregu.00768.2010.—We examined the transfer function of autonomic heart rate (HR) control in anesthetized sedentary and exercise-trained (16 wk, treadmill for 1 h, 5 times/wk at 15 m/min and 15-degree grade) rats for comparison to HR variability assessed in the conscious resting state. The transfer function from sympathetic stimulation to HR response was similar between groups (gain, 4.2 ± 1.5 vs. 4.5 ± 1.5 beats·min^{-1}·Hz^{-1}; natural frequency, 0.07 ± 0.01 vs. 0.08 ± 0.01 Hz; damping coefficient, 1.96 ± 0.55 vs. 1.69 ± 0.15; and lag time, 0.7 ± 0.1 vs. 0.6 ± 0.1 s; sedentary vs. exercise trained, respectively, means ± SD). The transfer gain from vagal stimulation to HR response was 6.1 ± 3.0 in the sedentary and 9.7 ± 5.1 beats·min^{-1}·Hz^{-1} in the exercise-trained group ($P = 0.06$). The corner frequency (0.11 ± 0.05 vs. 0.17 ± 0.09 Hz) and lag time (0.1 ± 0.1 vs. 0.2 ± 0.1 s) did not differ between groups. When the sympathetic transfer gain was averaged for very-low-frequency and low-frequency bands, no significant group effect was observed. In contrast, when the vagal transfer gain was averaged for very-low-frequency, low-frequency, and high-frequency bands, exercise training produced a significant group effect ($P < 0.05$ by two-way, repeated-measures ANOVA). These findings suggest that, in the frequency domain, exercise training augments the dynamic HR response to vagal stimulation but not sympathetic stimulation, regardless of the frequency bands.

heart rate variability; transfer function; systems analysis

HEART RATE VARIABILITY (HRV) is considered to be a useful noninvasive assessment of autonomic nervous system activity. It has been well recognized that exercise training increases HRV at rest (4, 19). A recent meta-analysis by Sandercock et al. (28) demonstrated that exercise training results in significant increases in R-R interval and high-frequency (HF) power of HRV. Nevertheless, not all studies have demonstrated increases in HRV after exercise training (7). To date, the exact mechanisms underlying increases in HRV after exercise training remain to be elucidated. Many earlier studies have suggested that the augmentation of HRV induced by exercise training may be caused by a withdrawal of sympathetic tonus and/or an increase in vagal tonus (5, 14, 36). Autonomic tone assessed by HRV may reflect both the autonomic outflow from the central nervous system and the peripheral autonomic regulation of atrial pacemaker cells. The latter can be assessed quantitatively by examining the heart rate (HR) response to electrical stimulation of the autonomic nerves. Furthermore, recent studies suggested that peripheral autonomic regulation of atrial pacemaker cells could contribute to the exercise training-induced increases in cardiac vagal function (9, 10).

Equivocal results, however, have been reported using autonomic nerve stimulation. Regarding the vagal system, the effects of exercise training have been inconsistent among studies, showing both increases (9, 10) and reductions in vagally stimulated HR control (25). When considering the sympathetic system, a previous study demonstrated that the HR response to sympathetic stimulation was reduced by exercise training (22). However, the mechanisms underlying the training effect are controversial (3, 15, 26, 29, 33, 35). These equivocal results could be explained by differences in species and modes of exercise training among studies (i.e., exercise type, intensity, and duration, etc.). More importantly, since these studies of autonomic nerve stimulation did not evaluate HRV, a causal relationship between increased HRV and adaptation in peripheral autonomic HR control remains largely undetermined. Furthermore, despite the fact that HRV has been evaluated by using frequency domain as well as time domain analyses, to date, there are no reports available examining the effects of exercise training on the dynamic HR response to sympathetic or vagal stimulation in the frequency domain. Analysis of peripheral autonomic regulation in the frequency domain would advance our understanding of the mechanisms responsible for the alterations in HRV that occur in response to exercise training.

We have recently developed a technique to assess the dynamic characteristics of HR control by the autonomic nervous system in rats using transfer function analysis (21). The transfer function analysis can quantitatively evaluate the HR response to autonomic nerve stimulation over a wide frequency range that is necessary for interpreting the generation of HRV. Therefore, the aims of the present study were *1*) to identify the dynamic characteristics of sympathetic and vagal HR control in exercised-trained rats and *2*) to determine whether alterations in peripheral autonomic regulation contribute to changes in the frequency components of HRV in exercised-trained rats.

MATERIALS AND METHODS

Animal Care and Training Program

Animal care was in accordance with the "Guiding Principles for Care and Use of Animals in the Field of Physiological Sciences," approved by the Physiological Society of Japan. All protocols were reviewed and approved by the Animal Subjects Committee of the

Address for reprint requests and other correspondence: M. Mizuno, Dept. of Physical Therapy, Univ. of Texas Southwestern Medical Center at Dallas, 5323 Harry Hines Blvd., Dallas, TX 75390-9174 (e-mail: masaki.mizuno@utsouthwestern.edu).

National Cerebral and Cardiovascular Center. Fourteen male Sprague-Dawley rats (200–250 g body wt) were fed standard laboratory chow and water ad libitum and housed three per cage in a temperature-controlled room with a 12:12-h dark-light cycle. Rats were randomly assigned to one of two groups: sedentary ($n = 7$) and exercise trained ($n = 7$).

Exercise training was performed on a motor-driven treadmill, 5 days/wk for 16 wk, gradually progressing toward a speed of 15 m/min at a 15-degree grade for 60 min. Sedentary rats walked (10 m/min at 15 degrees) 10 min/day once per week during the 16-wk period to maintain treadmill familiarity. At the end of the 16-wk period, maximal exercise capacity was measured twice in each rat in tests separated by 2 days (6). The protocol for the maximal exercise capacity test consisted of walking at 10 m/min for 5 min followed by 2 m/min increases in speed every 2 min until the rat reached exhaustion. Rats were considered exhausted when they failed to stay off of a shock bar.

Assessment of Autonomic Tone in the Conscious Resting State

After the performance test, three steel electrodes were implanted under anesthesia. These electrodes were utilized for monitoring the electrocardiogram. The R-R interval was measured using a cardiotachometer (model AT601G; Nihon Kohden, Tokyo, Japan). On the first day of the study, which was 24 h after electrodes had been implanted, resting HR was recorded to analyze the R-R interval variability in the quiet unrestrained rat that was kept in a small box. In accordance with a previous study (25), autonomic tone was assessed by intraperitoneal injections of methylatropine (3 mg/kg) and propranolol (4 mg/kg). Immediately after resting HR was recorded, methylatropine was injected. Since the HR response to methylatropine reached its peak in 10–15 min, this time interval was allocated before the HR measurement. Propranolol was injected after methylatropine injection, and again the HR was measured after 10–15 min. Intrinsic HR was evaluated after simultaneous blockade by propranolol and methylatropine. Sympathetic tonus was defined as the difference between the HR after methylatropine injection and intrinsic HR. On the second day, propranolol was administered first to obtain the inverse sequence of blockade. Vagal tonus was defined as the difference between the HR after propranolol injection and intrinsic HR.

Sympathetic and Vagal Stimulation

Surgical preparations. After obtaining data for the assessment of autonomic tone and HRV, rats were anesthetized by a mixture of urethane (250 mg/ml) and α-chloralose (40 mg/ml), initiated with an intraperitoneal bolus injection of 1 ml/kg. If additional anesthesia was needed, 0.1 ml/kg was given intraperitoneally. The rats were intubated and mechanically ventilated with oxygen-enriched room air. The rats were slightly hyperventilated to suppress chemoreflexes. A catheter was placed in the right femoral artery and connected to a pressure transducer (model DX-200; Nihon Kohden, Tokyo, Japan) to measure arterial pressure (AP). HR was measured using a cardiotachometer (model AT601G; Nihon Kohden) triggered by the R wave on the electrocardiogram. A catheter was introduced into the right femoral vein for drug administration. Sinoaortic barodenervation was performed bilaterally to minimize changes in sympathetic efferent nerve activity via arterial baroreflexes. The vagi were sectioned bilaterally at the neck. A pair of bipolar stainless steel electrodes was attached to the right cervical sympathetic nerve for efferent sympathetic stimulation or the right cervical vagus for efferent vagal stimulation. The stimulation electrodes and nerve were secured with silicon glue (Kwik-Sil; World Precision Instruments, Sarasota, FL). Body temperature was monitored with a thermometer placed in the rectum and was maintained at 38°C with a heating pad throughout the experiment.

Experimental procedures. The pulse duration was set at 2 ms and the stimulation amplitude was fixed at 10 V for both sympathetic and vagal nerve stimulation. To allow for stabilization of hemodynamics, sympathetic and vagal nerve stimulations were started ~1 h after the end of surgical preparations. Between sympathetic and vagal stimulation protocols > 15 min elapsed to allow AP and HR to return to their respective baseline values.

To estimate the dynamic transfer characteristics from sympathetic stimulation to HR response, the sectioned end of the right cervical sympathetic nerve was stimulated employing a frequency-modulated pulse train for 10 min. The stimulation frequency was switched every 1,000 ms to either 0 or 5 Hz according to a binary white noise signal. The power spectrum of the stimulation signal was reasonably constant up to 0.5 Hz. The transfer function was estimated up to 0.5 Hz because the reliability of estimation decreased due to the diminution of input power above this frequency. The selected frequency range sufficiently spanned the range of physiological interest (21). For estimation of the static transfer characteristics from sympathetic stimulation to HR response, stepwise sympathetic stimulation was performed. Sympathetic stimulation frequency was increased from 1 to 5 Hz in 1-Hz increments. Each frequency step was maintained for 60 s.

To estimate the dynamic transfer characteristics from vagal stimulation to HR response, the right vagus was stimulated employing a frequency-modulated pulse train for 10 min. The stimulation frequency was switched every 500 ms to either 0 or 10 Hz according to a binary white noise signal. The power spectrum of the stimulation signal was reasonably constant up to 1 Hz. The transfer function was estimated up to 1 Hz because the reliability of estimation decreased due to the diminution of input power above this frequency. The selected frequency range sufficiently spanned the range of physiological interest (21). For estimation of the static transfer characteristics from vagal stimulation to HR response, stepwise vagal stimulation was performed. Vagal stimulation frequency was changed among 2, 4, 8, 16, and 32 Hz. Each frequency step was maintained for 60 s.

Data Analysis

Spectral analysis of HRV. Data obtained during the conscious resting state were digitized at 200 Hz utilizing a 12-bit analog-to-digital converter and stored on the hard disk of a dedicated laboratory computer system. Beat-by-beat time series of the R-R interval were interpolated every 130 ms (Δt). Twelve data segments of 512 (N) points overlapping half of the preceding data were processed. For each data segment, after the linear trend was removed and the Hanning window applied, power spectral density was computed using the fast Fourier transform algorithm. The frequency resolution was $\Delta f = 1/(N\,\Delta t)$, i.e., 0.015 Hz, and the highest frequency was $\Delta f = 1/2\Delta t$, i.e., 3.85 Hz, where f is frequency. The very-low-frequency (VLF) band ranged between 0.017 and 0.27 Hz, the low-frequency (LF) band between 0.27 and 0.75 Hz, and the high-frequency (HF) band between 0.75 and 3.3 Hz, according to an earlier report (8). The percentage of LF or HF power relative to the sum of LF and HF powers and the ratio of LF to HF power were also calculated.

Transfer function analysis. The dynamic characteristics of the HR response to sympathetic or vagal stimulation were estimated by a transfer function analysis (see APPENDIX for details). Dynamic sympathetic control of HR was quantified by fitting a second-order low-pass filter with pure delay to the estimated transfer function. The dynamic vagal control of HR was quantified by fitting a first-order, low-pass filter with pure delay to the estimated transfer function. To facilitate the intuitive understanding of the system's dynamic characteristics, we calculated the system step response of HR to 1-Hz nerve stimulation as follows.

The system impulse response was derived from the inverse Fourier transform of the transfer function. The system step response was then obtained from the time integral of the impulse response. The length of the step response was 51.2 s. The 80% rise time for the sympathetic step response or the 80% fall time for the vagal step response was estimated as the time at which the step response reached 80% of the

Table 1. *Physical characteristics*

	Sedentary	Exercise Trained
Body weight, g	642 ± 33	534 ± 33*
Ventricular weight, g	1.22 ± 0.03	1.17 ± 0.04*
Ventricular weight/body weight, g/kg	1.9 ± 0.1	2.2 ± 0.1*
Lung weight, g	2.13 ± 0.27	1.89 ± 0.38
Lung weight/body weight, g/kg	3.3 ± 0.3	3.5 ± 0.7
Performance test, s	1150 ± 165	1790 ± 389*

Values are means ± SD. *$P < 0.05$ compared with sedentary group.

steady-state response calculated by averaging the last 10 s of data of the step response.

Statistical Analysis

All data are represented as means ± SD. Data were analyzed using unpaired Student's *t*-tests (sedentary vs. exercise trained) or two-way, repeated-measures ANOVA. Values of $P < 0.05$ were considered to be significant.

RESULTS

Physical Characteristic

Morphometric characteristics and exercise capacity for sedentary and exercised-trained rats are presented in Table 1. The mean body weight of the exercised-trained rats was significantly smaller than that of the sedentary rats. The mean ventricular weight of the exercised-trained rats was slightly but significantly smaller than that of the sedentary rats. Consequently, the ventricular weight normalized by body weight was significantly greater in the exercised-trained compared with the sedentary group. The lung weight-to-body weight ratio was not different between the groups. Exercise capacity was 64% greater in the exercised-trained than in the sedentary group. The reproducibility of measuring the maximal exercise capacity was reasonably high ($y = 1.2x - 226.1$, $R^2 = 0.79$; x and y represent the first and second measurements).

Spectral Analysis of HRV and Autonomic Tone in the Conscious Resting State

The power spectral densities of R-R interval are shown in Table 2. The percentage of LF power was significantly smaller, and the percentage of HF power was significantly greater in the exercised-trained rats than in the sedentary rats. The LF/HF ratio in the exercised-trained rats was significantly smaller compared with that in the sedentary rats. HR at rest was significantly lower in the exercised-trained compared with the sedentary group (Fig. 1*A*). The intrinsic HR was similar between the groups (Fig. 1*A*). Although the sympathetic tonus was comparable between the groups, the vagal tonus tended to be greater ($P = 0.08$) in the exercised-trained compared with the sedentary group (Fig. 1*B*).

Dynamic Sympathetic and Vagal Transfer Functions

Table 3 summarizes hemodynamics during dynamic sympathetic stimulation. Sympathetic stimulation significantly increased mean HR in both sedentary and exercised-trained groups. Mean HR and AP did not differ between the groups, before and during sympathetic stimulation. Figure 2*A* illustrates the dynamic transfer function characterizing sympathetic HR control. The frequency band effect was significant ($P < 0.0001$) but the group effect was insignificant ($P = 0.5461$) in the dynamic gain values of the sympathetic transfer function by two-way, repeated-measures ANOVA. The parameters of the sympathetic transfer function were comparable between the groups (Table 4). Figure 2*B* shows the calculated step response of HR to sympathetic stimulation. The steady-state response and the 80% rise time did not differ significantly between the groups (Table 4).

Table 5 summarizes hemodynamics during dynamic vagal stimulation. Vagal stimulation significantly decreased mean HR in both sedentary and exercised-trained groups. Mean HR and AP did not differ between the groups, before and during vagal stimulation. Figure 3*A* illustrates the dynamic transfer function characterizing vagal HR control. The frequency band effect ($P < 0.0001$) and the group effect ($P < 0.0001$) were both significant in the dynamic gain values of the vagal transfer function by two-way, repeated-measures ANOVA. The estimated dynamic gain (*see* APPENDIX) tended to be greater in the exercised-trained compared with the sedentary group ($P = 0.06$, Table 6). Other parameters did not differ between the groups. Figure 3*B* shows the calculated step response of HR to vagal stimulation. The calculated steady-state response in the exercised-trained rats also tended to be greater than that in the sedentary rats ($P = 0.06$, Table 6). There was no significant difference in the 80% fall time between the groups.

Dynamic Gain Values of Sympathetic and Vagal Transfer Function Corresponding to HRV Frequency Bands

When dynamic gain values of the sympathetic transfer function were averaged for the VLF and LF (up to 0.5 Hz, see METHODS) bands, the frequency band effect was significant, but the group effect was insignificant by two-way, repeated-measures ANOVA (Fig. 4*A*). When dynamic gain values of the vagal transfer function were averaged for the VLF, LF, and HF (up to 1 Hz, see METHODS) bands, the frequency band effect was insignificant but the group effect was significant such that the dynamic gain was significantly greater in the exercised-trained compared with the sedentary group (Fig. 4*B*).

Static Sympathetic and Vagal Transfer Function

The increase in HR with stepwise sympathetic stimulation was similar between groups (Fig. 5*A*). The stimulation frequency effect was significant, while the group effect was insignificant by two-way, repeated-measures ANOVA. In contrast, the decrease in HR with stepwise vagal stimulation was greater in the exercised-trained compared with sedentary rats (Fig. 5*B*). Both the stimulation frequency effect and the group effect were significant.

Table 2. *Spectral parameters of R-R interval*

	Sedentary	Exercise Trained
Variance, ms^2	87 ± 39	90 ± 32
VLF, ms^2	73 ± 30	80 ± 30
LF, ms^2	6.3 ± 3.4	3.1 ± 3.0
LF, %	49 ± 11	36 ± 7*
HF, ms^2	8.0 ± 7.6	6.2 ± 7.1
HF, %	51 ± 11	64 ± 7*
LF/HF ratio	1.0 ± 0.5	0.6 ± 0.2*

Values are means ± SD. LF, low frequency; VLF, very low frequency; HF, high frequency; *$P < 0.05$ compared with sedentary group.

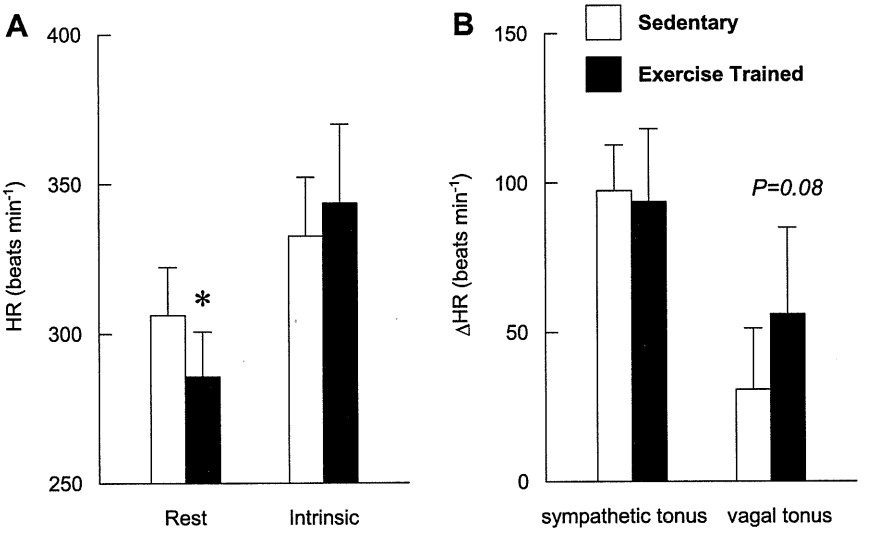

Fig. 1. Heart rate (HR) at rest and intrinsic HR (*A*) and HR sympathetic and vagal tone (*B*) obtained in sedentary and exercised-trained rats. *$P < 0.05$ compared with sedentary group.

DISCUSSION

We have examined the dynamic transfer function of autonomic HR control by using random binary sympathetic and vagal nerve stimulation in sedentary and exercised-trained rats. The major findings in the present study are *1*) that the exercise training did not alter the sympathetic transfer function substantially but augmented the dynamic gain of the vagal transfer function; and *2*) in the frequency domain, exercise training increased the dynamic HR response to vagal stimulation but not sympathetic stimulation, regardless of the frequency band. These findings are the first quantitative data on the effect of exercise training on the dynamic characteristics of peripheral HR control by the sympathetic and vagal systems.

Validity of Exercise Training

The relative ventricular hypertrophy and higher exercise capacity in the exercised-trained compared with the sedentary group suggested that exercise program used in the present study was sufficient to induce physiological adaptations commensurate with an effective training stimulus. As is well known, exercise training induces bradycardia at rest (Fig. 1*A*). Moreover, changes in the spectral parameters for R-R interval (Table 2) and autonomic tone (Fig. 1*B*) induced by the exercise training are consistent with earlier studies in rats (30, 31).

Effect of Exercise Training on Sympathetic and Vagal Transfer Function

Exercise training altered neither dynamic (Fig. 2) nor static sympathetic transfer function (Fig. 5*A*). These results are different than those reported in a previous study in which swim training significantly reduced the HR response to sympathetic nerve stimulation in a double atrial/right stellate ganglion preparation in guinea pigs (22). The discrepancy between investigations may have arisen from differences in the nerves experimentally stimulated (cervical sympathetic nerve vs. stellate ganglion), animal species studied (rats vs. guinea pigs), and/or experimental preparation utilized (in vivo vs. ex vivo). The mechanisms underlying the sympathetically mediated exercise training effect on HR are also controversial. For instance, chronotropic responsiveness to isoproterenol has been reported to be decreased in one study (15) but unchanged in another (22) by exercise training. Furthermore, in response to exercise training, the density and affinity of β-adrenoceptors in the heart have been shown to be reduced in some reports (26, 33), while unchanged in others (3, 34, 35).

Table 3. *Arterial pressure(AP) and heart rate (HR) during dynamic sympathetic stimulation protocol*

	Sedentary		Exercise Trained	
	Prestimulation	During Stimulation	Prestimulation	During Stimulation
AP, mmHg	74 ± 16	68 ± 15†	89 ± 17	84 ± 24
HR, beats/min	377 ± 25	444 ± 23†	381 ± 16	444 ± 26†

Values are means ± SD. †$P < 0.05$ compared with prestimulation.

Exercise training augmented the dynamic gain of the vagal transfer function (Fig. 2). The effect of exercise training was also significant for static vagal transfer function (Fig. 5*B*). These results are in agreement with previous studies showing that exercise training significantly augmented the HR response to vagal nerve stimulation in a double atrial/right vagal nerve preparation using mice (9, 10). In contrast, Negrao et al. (25) demonstrated that the HR response to vagal stimulation was depressed in exercised-trained rats. A possible explanation for this disparate result is that the arterial baroreflexes remained intact in the experimental preparation used in the study (25). In contrast, sinoaortic barodenervation was performed in the present investigation to minimize baroreflex-mediated changes in sympathetic efferent nerve activity. Exercise training has been shown to attenuate the baroreflex-mediated sympathetic nerve response to hypotension (11). Although speculative, in the study by Negrao et al. (25), baroreflex-mediated sympathetic activation in response to vagally-induced hypotension might have been less in exercised-trained compared with sedentary rats. Consequently, the gain of vagal stimulation might have been attenuated in exercised-trained animals relative to sedentary rats. This suggestion is reasonable given that accentuated antagonism is indicative of a diminution in background sym-

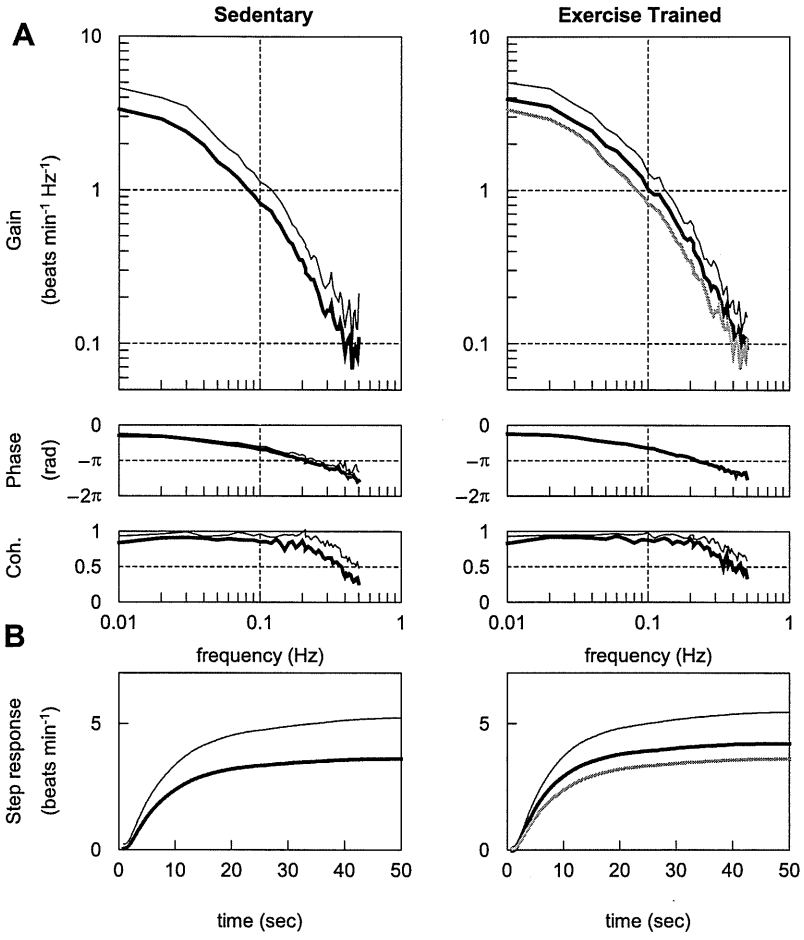

Fig. 2. *A*: transfer function from sympathetic stimulation to the HR response obtained in sedentary and exercised-trained rats. Gains (*top*), phase shifts (*middle*), and coherence (Coh.) functions (*bottom*) are presented. *B*: calculated step response to 1-Hz tonic sympathetic stimulation. Thick lines represent the mean, whereas thin lines indicate ± SD values. The gray solid curves in the gain and step response panels (*right*) duplicates the means (*left*).

pathetic tonus, which can decrease the gain of the vagal transfer function (17).

It has been documented that the intensity of exercise as well as the duration of exercise training are related to the autonomic adaptation to exercise training (28). These factors have been shown to be largely variable among different studies. A well-controlled experimental setup is needed to clarify these issues.

Dynamic Gain Values of Sympathetic and Vagal Transfer Functions Corresponding to HRV Frequency Bands

HRV is considered to reflect autonomic tone (19). The VLF component is likely to reflect changes in vasomotor tone in relation to thermoregulation and local adjustment of resistance in individual vascular beds; the LF component is considered to be a marker of sympathetic activity, although it remains a matter of debate; and the HF component mainly originates from respiratory activity and is considered to be mediated by vagal input (27). In rats, Cerutti et al. (8) determined that the LF component ranged between 0.27 and 0.74 Hz, and the HF component was > 0.75 Hz.

Averaged dynamic gain values of sympathetic transfer function for VLF and LF bands did not differ between the sedentary and exercised-trained groups (Fig. 4*A*). These results suggest that changes in the peripheral sympathetic control of HR likely do not contribute significantly to training-induced alterations in HRV. Therefore, the lower percentage of LF power and LF/HF ratio in the exercised-trained group (Table 2) may indicate reduced activation of sympathetic outflow from autonomic centers (23). In contrast, averaged dynamic gain values of vagal transfer function for VLF, LF, and HF bands (Fig. 4*B*) as

Table 4. *Sympathetic transfer function parameters and step response*

	Sedentary	Exercise Trained
Gain, beats·min^{-1}·Hz^{-1}	4.2 ± 1.5	4.5 ± 1.5
Natural frequency, Hz	0.07 ± 0.01	0.08 ± 0.01
Damping ratio	1.96 ± 0.55	1.69 ± 0.15
Lag time, s	0.71 ± 0.10	0.62 ± 0.11
Steady-state response, beats/min	3.6 ± 1.6	4.2 ± 1.2
80% rise time, s	12.9 ± 2.7	12.1 ± 3.0

Values are means ± SD. See APPENDIX for transfer function parameters.

Table 5. *AP and HR during dynamic vagal stimulation protocol*

	Sedentary		Exercise Trained	
	Prestimulation	During stimulation	Prestimulation	During stimulation
AP, mmHg	72 ± 21	68 ± 15	92 ± 14	80 ± 21
HR, beats/min	373 ± 18	327 ± 38 †	372 ± 14	301 ± 32 †

Values are means ± SD. †$P < 0.05$ compared with prestimulation.

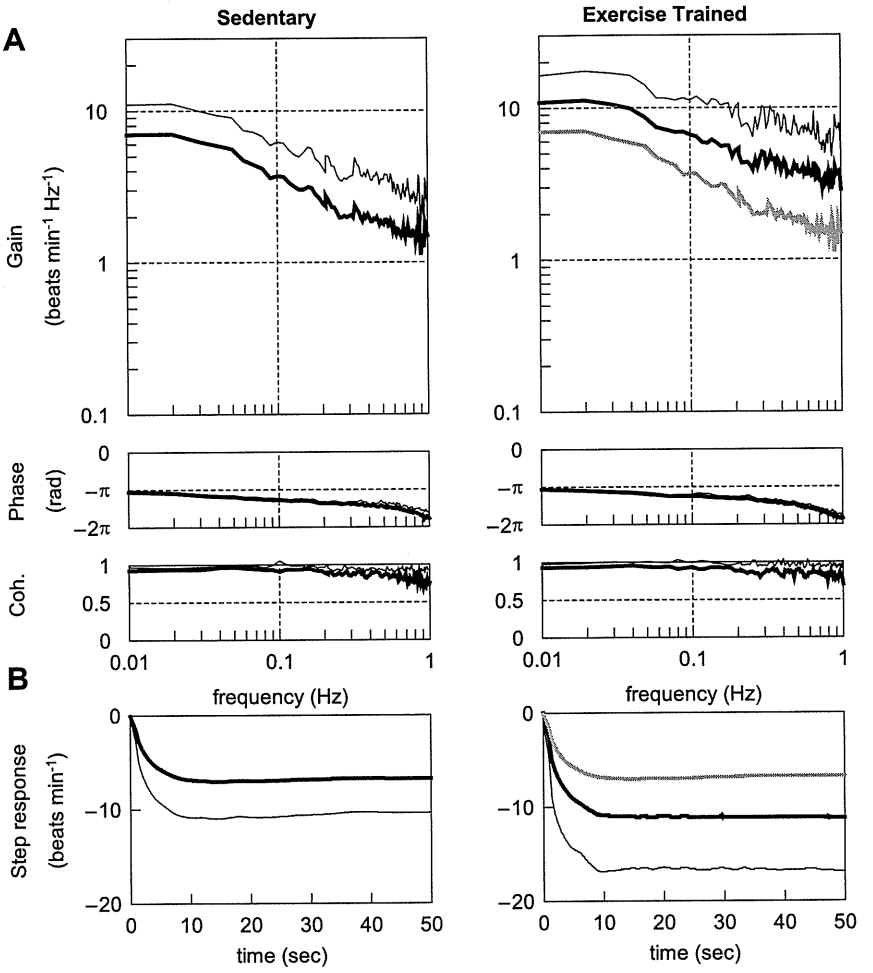

Fig. 3. *A*: transfer function from vagal stimulation to the HR response obtained in sedentary and exercised-trained rats. Gains (*top*), phase shifts (*middle*), and coherence functions (*bottom*) are presented. *B*: calculated step response to 1-Hz tonic vagal stimulation. Thick lines represent the mean, whereas thin lines indicate ± SD values. The gray solid curves in the gain and step response panels (*right*) duplicate the means (*left*).

well as the percentage of HF power (Table 2) were significantly greater in the exercised-trained compared with the sedentary group. These results suggest that the augmentation in HRV induced by exercise training is, at least in part, mediated by augmentations in the peripheral vagal control of HR.

What are the possible mechanisms underlying augmentations in the peripheral vagal control of HR? Danson and Paterson (10) have presented evidence that neuronal nitric oxide synthase may be a key enzymatic protein underlying such training-induced increases in cardiac vagal function. This group has also demonstrated that HR changes in response to vagal stimulation are enhanced by exercise training in wild-type mice but not in heterozygous neuronal nitric oxide synthase knockout mice (9). Another candidate for augmentations in the peripheral vagal control of HR is muscarinic receptors, which play a fundamental role in HR control via vagally mediated regulation. However, the effects of exercise training have been inconsistent among studies, showing both increases (12) and no change (2, 3) in muscarinic receptors in the myocardium of rats. The possibility cannot be dismissed that training-induced changes in the activity of afferent inputs mediating vagal outflow may also contribute to the alterations in HRV (4). Further investigation is needed to clarify these issues.

Table 6. *Vagal transfer function parameters and step response*

	Sedentary	Exercise Trained
Gain, beats·min^{-1}·Hz^{-1}	6.1 ± 3.0	9.7 ± 5.1#
Corner frequency, Hz	0.11 ± 0.05	0.17 ± 0.09
Lag time, s	0.10 ± 0.08	0.17 ± 0.08
Steady-state response, beats/min	−6.7 ± 3.6	−11.2 ± 5.7#
80% Fall time, s	4.3 ± 2.2	4.3 ± 1.5

Values are means ± SD. #P = 0.06 compared with sedentary group. See APPENDIX for transfer function parameters.

Perspectives and Significance

To date, the mechanisms underlying increased HRV after exercise training remain to be elucidated. HRV may reflect both the autonomic outflow from the central nervous system and the peripheral autonomic regulation of atrial pacemaker cells. In human studies, it is difficult to separately examine each factor. The findings of the present study suggest that the augmentation in HRV induced by exercise training is, at least in part, mediated by augmentations in the peripheral vagal control of HR. In other words, even if vagal outflow from the central nervous system remains unchanged after exercise training, HRV could be increased by an enhanced responsiveness in the peripheral vagal, but not sympathetic, regulation of HR.

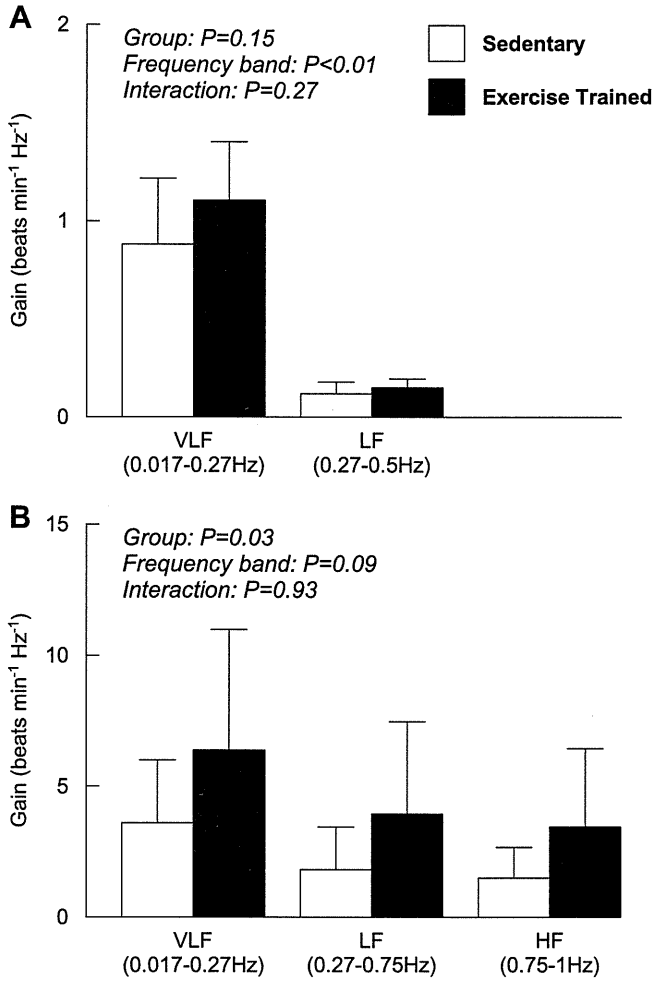

Fig. 4. Averaged sympathetic (*A*) and vagal (*B*) gain calculated from corresponding transfer function in very low frequency (VLF), low frequency (LF), and high frequency (HF) bands.

It has been well documented that decreased HRV is observed in heart failure (18) as well as in a variety of lifestyle-related diseases such as diabetes (16), hypertension (24), and obesity (1). Furthermore, reductions in HRV are related to increases in mortality rates as well as the occurrence of adverse cardiac events (32). Exercise training-induced augmentations in HRV maintain the potential to partially correct or normalize the autonomic dysfunction manifest in these disease states (4). Understanding the mechanisms contributing to the alterations in HRV induced by exercise training may significantly impact the development of novel therapeutic strategies for the treatment of autonomic dysfunction.

Limitations

There are several limitations to this study. First, the rats were slightly hyperventilated throughout the stimulation protocol. We cannot rule out the possibility that the hyperventilation might have affected the results reported. Second, dynamic sympathetic stimulation lowered mean AP in sedentary rats although sinoaortic barodenervation was performed. This may be explained by a possible difference in left ventricular functional capacity. For example, under conditions of equivalent HR, changes in systolic blood pressure were smaller in sedentary rats compared with exercised-trained rats (13). Third, the stimulation amplitude was fixed at 10 V for both sympathetic and vagal nerve stimulation. It should be noted, however, that our preliminary results indicated that 10 V was sufficiently large enough to evoke maximal HR responses. Fourth, transfer function data were obtained from anesthetized animals. This must be taken into account when interpreting the present results as anesthesia may affect the peripheral autonomic regulation of atrial pacemaker cells. Finally, we stimulated the sympathetic and vagal nerves according to a binary white noise signal. Although this method of stimulation is quite different from the physiological pattern of neuronal discharge, the coherence was near unity over the frequency range of interest. This finding indicates that the system properties do not vary considerably in response to different patterns of stimulation.

Conclusion

In the present study, it was demonstrated for the first time that exercise training did not alter dynamic sympathetic control of HR, while it did augment dynamic vagal control of HR. In addition, the group effect was significant with regard to the dynamic gain values for the vagal transfer functions corresponding to VLF, LF, and HF bands. This finding suggests that enhancements in the peripheral vagal control of HR may, at

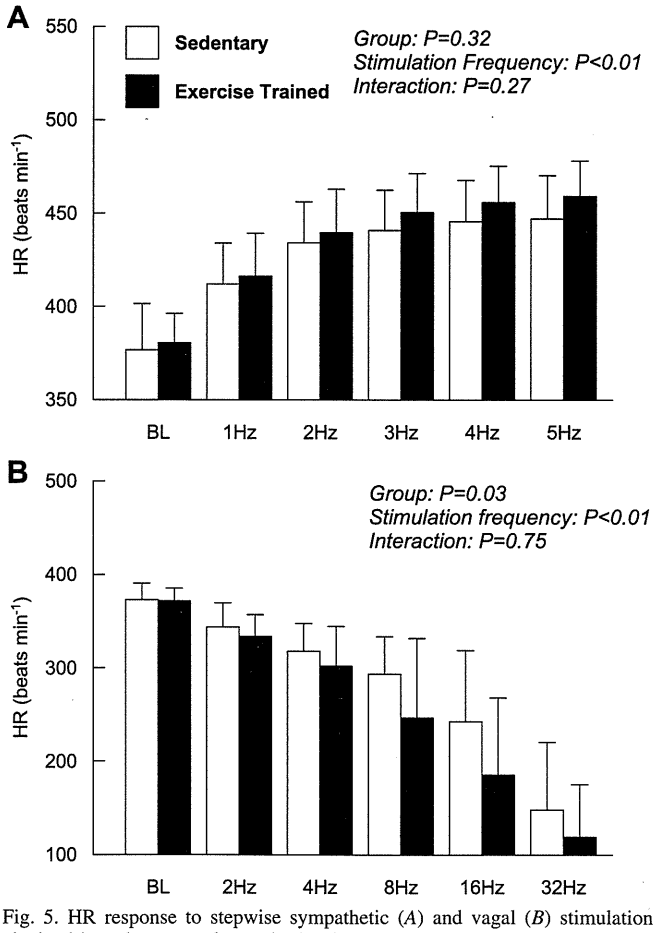

Fig. 5. HR response to stepwise sympathetic (*A*) and vagal (*B*) stimulation obtained in sedentary and exercised-trained rats.

least in part, contribute to the exercise-induced augmentation in HRV in healthy rats.

APPENDIX: TRANSFER FUNCTION ANALYSIS

The dynamic transfer function from binary white noise stimulation to the HR response was estimated based on the following procedure. Input-output data pairs of the stimulation frequency and HR were resampled at 10 Hz to be consistent with our previous study (21). Subsequently, data pairs were partitioned into eight 50% overlapping segments consisting of 1,024 data points each. For each segment, the linear trend was subtracted and a Hanning window was applied. A fast Fourier transform was then performed to obtain the frequency spectra of nerve stimulation [$N(f)$] and HR [$HR(f)$]. Over the eight segments, the power of the nerve stimulation [$S_{N\cdot N}(f)$], the power of the HR [$S_{HR\cdot HR}(f)$], and the cross-power between these two signals [$S_{N\cdot HR}(f)$] were ensemble averaged. Finally, the transfer function [$H(f)$] from nerve stimulation to the HR response was determined using the following equation (20).

$$H(f) = \frac{S_{N\text{-}HR}(f)}{S_{N\cdot N}(f)}$$

To quantify the linear dependence of the HR response on vagal or sympathetic stimulation, the magnitude-squared coherence function [$\mathrm{Coh}(f)$] was estimated employing the following equation (20).

$$\mathrm{Coh}(f) = \frac{|S_{\mathrm{N\text{-}HR}}(f)|^2}{S_{\mathrm{N\cdot N}}(f) \cdot S_{\mathrm{HR\cdot HR}}(f)}$$

Coherence values range from zero to unity. Unity coherence indicates perfect linear dependence between the input and output signals; in contrast, zero coherence indicates total independence between the two signals.

Since the transfer function from sympathetic stimulation to HR response in rats approximated a second order low-pass filter with pure delay (21), we determined the parameters of the sympathetic transfer function using the following equation.

$$H(f) = \frac{K}{1 + 2\zeta\frac{f}{f_N}j + \left(\frac{f}{f_N}j\right)^2} e^{-2\pi f j L}$$

where K is dynamic gain (in beats·min^{-1}·Hz^{-1}), f_N is the natural frequency (in Hz), ζ is the damping ratio, L is lag time (in s), and f and j represent frequency and imaginary units, respectively. These parameters were estimated by means of an iterative nonlinear least squares regression.

Since the transfer function from vagal stimulation to HR response in rats approximated a first-order, low-pass filter with pure delay (21), we determined the parameters of the vagal transfer function using the following equation.

$$H(f) = \frac{-K}{1 + \frac{f}{f_C}j} e^{-2\pi f j L}$$

where K represents the dynamic gain (in beats·min^{-1}·Hz^{-1}), f_C denotes the corner frequency (in Hz), L denotes the lag time (in s), and f and j represent frequency and imaginary units, respectively. The negative sign in the numerator indicates the negative HR response to vagal stimulation. These parameters were estimated by means of an iterative nonlinear least squares regression.

GRANTS

This study was supported by Health and Labor Sciences Research Grants H18-nano-Ippan-003, H19-nano-Ippan-009, H20-katsudo-Shitei-007, and H21-nano-Ippan-005 from the Ministry of Health, Labor and Welfare of Japan, by Grants-in-Aid for Scientific Research No. 19700559 from the Ministry of Education, Culture, Sports, Science and Technology in Japan, and by the Industrial Technology Research Grant Program from New Energy and Industrial Technology Development Organization of Japan. M. Mizuno was supported from Research Fellowships of the Japan Society for the Promotion of Science for Young Scientists.

DISCLOSURES

No conflicts of interest, financial or otherwise, are declared by the author(s).

REFERENCES

1. **Arone LJ, Mackintosh R, Rosenbaum M, Leibel RL, Hirsch J.** Autonomic nervous system activity in weight gain and weight loss. *Am J Physiol Regul Integr Comp Physiol* 269: R222–R225, 1995.
2. **Barbier J, Rannou-Bekono F, Marchais J, Berthon PM, Delamarche P, Carre F.** Effect of training on β1-, β2-, β3-adrenergic and M2 muscarinic receptors in rat heart. *Med Sci Sports Exerc* 36: 949–954, 2004.
3. **Barbier J, Reland S, Ville N, Rannou-Bekono F, Wong S, Carre F.** The effects of exercise training on myocardial adrenergic and muscarinic receptors. *Clin Auton Res* 16: 61–65, 2006.
4. **Billman GE.** Cardiac autonomic neural remodeling and susceptibility to sudden cardiac death: effect of endurance exercise training. *Am J Physiol Heart Circ Physiol* 297: H1171–H1193, 2009.
5. **Blomqvist CG, Saltin B.** Cardiovascular adaptations to physical training. *Annu Rev Physiol* 45: 169–189, 1983.
6. **Brenner DA, Apstein CS, Saupe KW.** Exercise training attenuates age-associated diastolic dysfunction in rats. *Circulation* 104: 221–226, 2001.
7. **Buch AN, Coote JH, Townend JN.** Mortality, cardiac vagal control and physical training–what's the link? *Exp Physiol* 87: 423–435, 2002.
8. **Cerutti C, Gustin MP, Paultre CZ, Lo M, Julien C, Vincent M, Sassard J.** Autonomic nervous system and cardiovascular variability in rats: a spectral analysis approach. *Am J Physiol Heart Circ Physiol* 261: H1292–H1299, 1991.
9. **Danson EJ, Mankia KS, Golding S, Dawson T, Everatt L, Cai S, Channon KM, Paterson DJ.** Impaired regulation of neuronal nitric oxide synthase and heart rate during exercise in mice lacking one nNOS allele. *J Physiol* 558: 963–974, 2004.
10. **Danson EJ, Paterson DJ.** Enhanced neuronal nitric oxide synthase expression is central to cardiac vagal phenotype in exercise-trained mice. *J Physiol* 546: 225–232, 2003.
11. **DiCarlo SE, Bishop VS.** Exercise training attenuates baroreflex regulation of nerve activity in rabbits. *Am J Physiol Heart Circ Physiol* 255: H974–H979, 1988.
12. **Favret F, Henderson KK, Clancy RL, Richalet JP, Gonzalez NC.** Exercise training alters the effect of chronic hypoxia on myocardial adrenergic and muscarinic receptor number. *J Appl Physiol* 91: 1283–1288, 2001.
13. **Fitzsimons DP, Bodell PW, Herrick RE, Baldwin KM.** Left ventricular functional capacity in the endurance-trained rodent. *J Appl Physiol* 69: 305–312, 1990.
14. **Goldsmith RL, Bigger JT Jr, Steinman RC, Fleiss JL.** Comparison of 24-hour parasympathetic activity in endurance-trained and untrained young men. *J Am Coll Cardiol* 20: 552–558, 1992.
15. **Hammond HK, White FC, Brunton LL, Longhurst JC.** Association of decreased myocardial β-receptors and chronotropic response to isoproterenol and exercise in pigs following chronic dynamic exercise. *Circ Res* 60: 720–726, 1987.
16. **Ikeda T, Matsubara T, Sato Y, Sakamoto N.** Circadian blood pressure variation in diabetic patients with autonomic neuropathy. *J Hypertens* 11: 581–587, 1993.
17. **Kawada T, Ikeda Y, Sugimachi M, Shishido T, Kawaguchi O, Yamazaki T, Alexander J Jr, Sunagawa K.** Bidirectional augmentation of heart rate regulation by autonomic nervous system in rabbits. *Am J Physiol Heart Circ Physiol* 271: H288–H295, 1996.
18. **La Rovere MT, Pinna GD, Maestri R, Mortara A, Capomolla S, Febo O, Ferrari R, Franchini M, Gnemmi M, Opasich C, Riccardi PG, Traversi E, Cobelli F.** Short-term heart rate variability strongly predicts sudden cardiac death in chronic heart failure patients. *Circulation* 107: 565–570, 2003.

19. **Malliani A, Pagani M, Lombardi F, Cerutti S.** Cardiovascular neural regulation explored in the frequency domain. *Circulation* 84: 482–492, 1991.
20. **Marmarelis P, Marmarelis V.** The white noise method in system identification. In: *Analysis of Physiological Systems*. New York: Plenum, 1978, p. 131–221.
21. **Mizuno M, Kawada T, Kamiya A, Miyamoto T, Shimizu S, Shishido T, Smith SA, Sugimachi M.** Dynamic characteristics of heart rate control by the autonomic nervous system in rats. *Exp Physiol* 95: 919–925, 2010.
22. **Mohan RM, Choate JK, Golding S, Herring N, Casadei B, Paterson DJ.** Peripheral pre-synaptic pathway reduces the heart rate response to sympathetic activation following exercise training: role of NO. *Cardiovasc Res* 47: 90–98, 2000.
23. **Mueller PJ.** Exercise training attenuates increases in lumbar sympathetic nerve activity produced by stimulation of the rostral ventrolateral medulla. *J Appl Physiol* 102: 803–813, 2007.
24. **Mussalo H, Vanninen E, Ikaheimo R, Laitinen T, Laakso M, Lansimies E, Hartikainen J.** Heart rate variability and its determinants in patients with severe or mild essential hypertension. *Clin Physiol* 21: 594–604, 2001.
25. **Negrao CE, Moreira ED, Santos MC, Farah VM, Krieger EM.** Vagal function impairment after exercise training. *J Appl Physiol* 72: 1749–1753, 1992.
26. **Nieto JL, Laviada ID, Guillen A, Haro A.** Adenylyl cyclase system is affected differently by endurance physical training in heart and adipose tissue. *Biochem Pharmacol* 51: 1321–1329, 1996.
27. **Pagani M, Lombardi F, Guzzetti S, Rimoldi O, Furlan R, Pizzinelli P, Sandrone G, Malfatto G, Dell'Orto S, Piccaluga E.** Power spectral analysis of heart rate and arterial pressure variabilities as a marker of sympatho-vagal interaction in man and conscious dog. *Circ Res* 59: 178–193, 1986.
28. **Sandercock GR, Bromley PD, Brodie DA.** Effects of exercise on heart rate variability: inferences from meta-analysis. *Med Sci Sports Exerc* 37: 433–439, 2005.
29. **Schwarz P, Diem R, Dun NJ, Forstermann U.** Endogenous and exogenous nitric oxide inhibits norepinephrine release from rat heart sympathetic nerves. *Circ Res* 77: 841–848, 1995.
30. **Souza SB, Flues K, Paulini J, Mostarda C, Rodrigues B, Souza LE, Irigoyen MC, De Angelis K.** Role of exercise training in cardiovascular autonomic dysfunction and mortality in diabetic ovariectomized rats. *Hypertension* 50: 786–791, 2007.
31. **Tezini GC, Silveira LC, Villa-Cle PG Jr, Jacinto CP, Di Sacco TH, Souza HC.** The effect of aerobic physical training on cardiac autonomic control of rats submitted to ovariectomy. *Menopause* 16: 110–116, 2009.
32. **Tsuji H, Larson MG, Venditti FJ Jr, Manders ES, Evans JC, Feldman CL, Levy D.** Impact of reduced heart rate variability on risk for cardiac events. The Framingham Heart Study. *Circulation* 94: 2850–2855, 1996.
33. **Werle EO, Strobel G, Weicker H.** Decrease in rat cardiac β1- and β2-adrenoceptors by training and endurance exercise. *Life Sci* 46: 9–17, 1990.
34. **Williams RS.** Physical conditioning and membrane receptors for cardioregulatory hormones. *Cardiovasc Res* 14: 177–182, 1980.
35. **Williams RS, Schaible TF, Bishop T, Morey M.** Effects of endurance training on cholinergic and adrenergic receptors of rat heart. *J Mol Cell Cardiol* 16: 395–403, 1984.
36. **Yamamoto K, Miyachi M, Saitoh T, Yoshioka A, Onodera S.** Effects of endurance training on resting and post-exercise cardiac autonomic control. *Med Sci Sports Exerc* 33: 1496–1502, 2001.

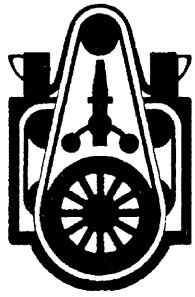

Heart Vessels (2011) 26:267–273
DOI 10.1007/s00380-010-0054-8

ORIGINAL ARTICLE

Effects of various doses of aspirin on platelet activity and endothelial function

Takashi Furuno · Fumiyasu Yamasaki · Takeshi Yokoyama · Kyoko Sato · Takayuki Sato · Yoshinori Doi · Tetsuro Sugiura

Received: 21 April 2009 / Accepted: 23 April 2010 / Published online: 10 November 2010

Abstract Although aspirin has become an established medicine for cardiac and cerebrovascular diseases, the optimal dose remains unknown. We evaluated the optimal dose of aspirin on platelet activity and endothelial function by administering 11 healthy male volunteers (32 ± 6 years of age) doses of aspirin that were increased in a stepwise manner (0, 81, 162, 330 and 660 mg/day) every 3 days. Platelet activity was assessed as surface P-selectin expression (%) measured by flow cytometry and the platelet aggregation ratio. Endothelial function in the brachial artery was assessed by measuring flow-mediated dilation (FMD) before and after reactive hyperemia. Platelet aggregation and P-selectin expression were significantly and dose-dependently suppressed (81–660 mg), and the FMD ratio tended to increase from 0 to 162 mg, but decreased significantly at 660 mg. In conclusion, although aspirin suppressed platelet activity and even surface P-selectin expression, higher doses worsened endothelial-mediated arterial dilation.

T. Furuno · K. Sato · Y. Doi
Medicine and Geriatrics, Kochi Medical School,
Nankoku, Kochi 783-8505, Japan

F. Yamasaki (✉) · T. Sugiura
Clinical Laboratory, Kochi Medical School,
Nankoku, Kochi 783-8505, Japan
e-mail: yamasakf-kochimed@umin.net

T. Yokoyama
Anesthesiology, Kochi Medical School,
Nankoku, Kochi 783-8505, Japan

T. Sato
Cardiovascular Control, Kochi Medical School,
Nankoku, Kochi 783-8505, Japan

Keywords Aspirin dose · Platelet activity · Endothelial function · Flow-mediated dilation

Introduction

Aspirin is established as a primary and secondary antiplatelet treatment for cardiovascular disease [1–5]. The recommended long-term daily dose of aspirin is 75–150 mg, which is considered to be at least as effective as higher doses [6]. Reports have indicated that higher doses of aspirin are ineffective because of bleeding complications [7–9] and impaired endothelial function [10–12]. Aspirin inhibits the synthesis of thromboxane A2 in platelets and of prostaglandin I2 in endothelial cells. Low dose aspirin only inhibits thromboxane A2 in platelets, whereas a high dose inhibits both. The inhibition of prostaglandin I2 synthesis in endothelial cells would increase the incidence of thromboembolic events [10–12]. However, the effects of optimal doses of aspirin on simultaneous platelet activation and endothelial function in humans remain obscure. One reason for this is that although platelet activation can be evaluated using the platelet aggregation test, a clinical method to evaluate prostaglandin I2 inhibition in endothelial cells remains to be established.

Endothelial function has recently been evaluated as flow-mediated dilation before and after reactive hyperemia [13], and endothelial dysfunction is apparent in patients with cardiovascular and metabolic diseases [14–19]. Although flow-mediated dilation after reactive hyperemia is mainly mediated by NO synthesized in the endothelia [20, 21], another pathway associated with prostacyclin and thromboxane A2 mediates vascular reactivity [22–24]. High dose of aspirin could affect this pathway, leading to vascular relaxation. The present study examines the effects

of various doses of aspirin on platelet activity and endothelial function in healthy humans to determine the optimal dose of aspirin required to suppress platelet aggregation and function.

Subjects and methods

Subjects

We enrolled 11 healthy male volunteers, aged 23–39 years (mean = 32 ± 6 years), with no evidence of heart disease according to a physical examination, standard 12-lead electrocardiography, chest radiography and echocardiography. None of the participants had hypertension, hypercholesteremia, diabetes mellitus or renal disease. All were in sinus rhythm and had not taken any medication for at least 14 days. Each of them provided written, informed consent to participate in the study, the protocol for which was approved by the Local Ethics Committee of Kochi Medical School.

Study protocol

Doses of aspirin (Bufferin 81 or 330 mg/tablet, Lion Co.) were increased (0, 81, 162, 330 and 660 mg) in a stepwise fashion every 3 days for 13 days. Platelet activation and endothelial function were measured at 11:00 a.m. before taking aspirin on the last day of each dose. The participants laid on a bed in a temperature-controlled quiet room, and venous blood was withdrawn from the left forearm vein. Endothelial function was measured in the right arm 30 min after blood collection. The participants did not exercise, consume beverages containing caffeine, high-fat foods or vitamin C, or use tobacco products for at least 4 h before the study.

Endothelial function

Endothelial function was assessed in the brachial artery by measuring flow-mediated dilation before and after reactive hyperemia. Data acquisition and analysis proceeded as described [13]. Briefly, the brachial artery of the right arm was imaged by high-resolution ultrasound (Acuson Sequoia 512) with a 10-MHz linear probe supported by a stereotactic clamp. We selected the B mode longitudinal section of the distal brachial artery, and the M-mode image was magnified using a resolution box function. Vertical internal diameter at end diastole gated by ECG was measured at rest for baseline. A tourniquet placed distally around the ipsilateral forearm was inflated to 250 mmHg for 4.5 min to induce reactive hyperemia. After rapid release, the inner diameter was measured 55 s later. The diameter was measured before and after hyperemia. The FMD ratio (%) was calculated as: 100 × (after diameter − before diameter)/before diameter. Scans were stored and analyzed by two independent observers.

Platelet aggregation test

Platelet function was determined as maximal platelet aggregation rate; that is, platelet-rich-plasma (PRP) was prepared from each participant. To minimize platelet activation during blood collection, blood was withdrawn using a 21-G butterfly needle without a tourniquet. The first 2 ml of blood was discarded, and then 20 ml of blood was transferred into polypropylene tubes containing sodium citrate (3.8%, 1 volume for 9 volumes of blood). We then prepared PRP by centrifugation at $120\times g$ for 10 min at room temperature. Platelet-poor plasma for control to compare PRP aggregation was obtained after re-centrifugation at $1{,}710\times g$ for 15 min.

Platelet aggregation was induced by adenosine diphosphate (ADP) (final concentration of 1.0 or 5.0 μmol/l, MC Medical, Tokyo, Japan) or by collagen (final concentration of 0.25 or 2 μg/ml, MC Medical). The time course of % transmission was measured (MCM HEMA TRACER 212TM; MC Medical), and the maximal platelet aggregation rate was calculated [25, 26].

Measurements of P-selectin (CD62P) and PNC levels

Samples were prepared, and levels of platelet P-selectin (CD62P) and PNC were measured as described [27, 28]. The sample used was the same blood that was collected for the platelet aggregation test. After the first 2 ml of blood was discarded, 2 ml of blood was collected and immediately added to 200 μl of sodium citrate (3.13%). All antibodies were purchased as follows: Fluorescein isothiocyanate (FITC) labeled IgG1 anti-CD62P from Dainippon Pharmaceutical, Osaka; phycoerythin (PE) labeled IgG2a anti-CD42b and FITC labeled IgG1 anti-CD11b from Beckman Coulter, Fullerton. As negative controls, FITC labeled IgG1 (Beckman Coulter, Fullerton) and double-stained (FITC/PE) IgG1 and IgG2a (Dako, High Wycombe) irrelevant antibodies were included. Blood samples were analyzed (EPICS XL Profile Flow Cytometer, Coulter, Miami, FL) using either one or two fluorochromes.

To prepare samples for measurements of platelet CD62P levels, blood (5 μl) was added to round-bottomed polystyrene tubes containing 50 μl platelet buffer (10 mmol/l HEPES, 145 mmol/l NaCl, 5 mmol/l KCl, 1 mmol/l $MgSO_4$, pH 7.4), and 5 μl of anti-CD62P or control IgG1 antibody. The samples were gently suspended and incubated in the dark at room temperature for 20 min without stirring. Then 250-μl fixative (Beckman Coulter, Fullerton,

9.25% formaldehyde) was added, and the tubes were incubated for a further 10 min. The samples were then diluted with 500 μl of buffer and analyzed by flow cytometry within 1 h of fixation. In flow cytometric analysis, the peaks emission intensity of FITC and phycoerythrin fluorescence were detected at 515 and 580 nm, respectively. After forward and side scatter was measured with the gain setting in logarithmic mode, platelet sized events were counted. CD62P positive platelets were defined as those with a fluorescence intensity exceeding that of 98% of the platelets stained with control antibody.

To prepare samples for the PNC measurements, blood (50 μl) was added to round-bottomed polystyrene tubes containing 5 μl each of anti-CD42b and anti-CD11b (platelet and neutrophil markers, respectively) or isotype control antibodies. The samples were gently mixed and incubated in the dark at room temperature for 10 min without stirring. Then 500 μl of fixative was added, and the tubes were incubated for a further 10 min. Flow cytometry proceeded within 1 h of preparation. After forward and side scatter were measured with the gain setting in linear mode, neutrophil-sized events were selected. Results were defined as positive when the fluorescence intensity exceeded that of the isotype matched (IgG1 and IgG2a) control antibody staining (98%). Both CD11b and CD42b positive events that were considered PNCs were expressed as ratios (%) of events with positive CD11b staining of those of whole neutrophils. We evaluated the ability of the platelets to be activated, i.e., platelet activation reserve in the presence of 5 μl of ADP (5 μmol/l).

We also counted blood cells and measured coagulation factors of prothrombin time (PT), activated partial thromboplastin time (APTT) and fibrinogen.

Statistical analysis

Data are presented as means ± SEM. Group means for each parameter were determined and compared using the analysis of variance (ANOVA) repeated measures, with the post-hoc Tukey–Kramer test. A value of $p < 0.05$ was considered to represent statistical significance.

Results

Aspirin administration did not alter the white blood cells, red blood cells, hemoglobin, hematocrit or platelet counts in the blood. The coagulation factors, PT and APTT, did not change significantly before and after aspirin administration. However, maximal platelet aggregation rates in the presence of ADP (5.0 μmol/l) or collagen (2 μg/ml) were significantly reduced from the baseline level after all doses of aspirin (81, 162, 330 and 660 mg): ADP; 78 ± 3–67 ± 2, 66 ± 2, 65 ± 2, 66 ± 2%, all ps < 0.01; collagen; 85 ± 2–34 ± 6, 38 ± 6, 34 ± 5, 35 ± 6%, all ps < 0.01. The effects on P-selectin, P-selectin with ADP and PNC with ADP tended to be similar (Table 1; Fig. 1), whereas PNC showed no tendency. Therefore, aspirin of any dose over 81 mg/day suppressed platelet activity.

Blood pressure was 121 ± 8/68 ± 8 at baseline and 127 ± 9/71 ± 8 at the end of the study, showing no significant change. At any dose of aspirin, heart rate at each measurement of FMD did not change significantly. Although arterial diameter did not significantly change after hyperemia, the FMD ratio (%) tended to increase at a dose of 81 mg (1.68 ± 0.29–2.78 ± 0.47, $p = 0.08$) and significantly increased at 162 mg (3.67 ± 0.41, $p < 0.05$) compared with the baseline without aspirin. The FMD ratio then tended to decrease at a dose of 330 mg (3.30 ± 0.50, n.s.) from 162 mg, but tended to be higher compared with the baseline ($p = 0.07$). The FMD ratio further decreased at a dose of 660 mg (1.07 ± 0.34) compared with that at either 162 or 330 mg ($p < 0.01$, $p < 0.01$, respectively), and tended to be lower from baseline or at a dose of 81 mg (Table 1; Fig. 1). Therefore, the optimal dose of aspirin for endothelial function assessed by the FMD ratio was 162 mg per day.

Discussion

The major finding of this study was that aspirin at any daily dose over 81 mg suppressed platelet activity and that the optimal dose of endothelial function was 162 mg/day. However, 660 mg/day of aspirin worsened endothelial function.

Aspirin plays an important role in the primary and secondary prevention of cardiovascular events, and it has remained the most cost-effective clinical drug for over 3 decades [1–6]. Reports indicate that a daily dose of 75–150 mg is just as effective as higher doses. An initial loading dose of at least 150 mg aspirin might be required in acute settings, but the effects of daily doses of <75 mg have been less certain, and doses of >1,000 mg daily are not recommended due to bleeding side effects [7–9].

The recent findings of the Antithrombotic Trialists' Collaboration meta-analysis of patients with previous thrombotic events or other predisposing conditions showed that aspirin reduces the total risk for cardio-cerebral vascular events by 22% [6]. From the viewpoint of the daily aspirin dose, the proportional reduction in vascular events was 19% at 500–1,500 mg/day, 26% at 160–325 mg/day and 32% at 75–150 mg/day. Although the effects of aspirin doses of ≥ or <75 mg in a direct comparison did not significantly differ, doses of <75 mg/day seemed to have somewhat reduced

Table 1 Blood cell count, coagulation factor, platelet activity and endothelial function

Aspirin dose (mg/day)	0	81	162	330	660
Blood cell count					
RBC ($\times 10^4/\mu l$)	490 ± 7	483 ± 10	483 ± 8	483 ± 8	486 ± 7
Hemoglobin (g/dl)	15.2 ± 0.1	15.2 ± 0.2	14.9 ± 0.2	15.0 ± 0.2	14.7 ± 0.2
Hematocrit (%)	44.5 ± 0.3	44.6 ± 0.5	43.8 ± 0.6	44.3 ± 0.6	43.1 ± 0.6
Platelet ($\times 10^4/\mu l$)	26.5 ± 1.4	25.1 ± 1.0	24.3 ± 0.9	24.6 ± 1.1	24.7 ± 0.9
WBC (μl^{-1})	5.70 ± 0.42	5.84 ± 0.34	5.84 ± 0.34	5.74 ± 0.34	6.29 ± 0.56
Coagulation factor					
PT (s)	10.4 ± 0.1	10.3 ± 0.1	10.3 ± 0.1	10.2 ± 0.1	10.1 ± 0.1
PT (%)	95.7 ± 4.0	98.3 ± 5.1	96.3 ± 3.3	99.7 ± 3.1	105.2 ± 5.4
INR	1.03 ± 0.03	1.02 ± 0.03	1.03 ± 0.02	1.01 ± 0.02	0.98 ± 0.03
APTT (s)	28.1 ± 0.8	27.8 ± 0.5	27.8 ± 0.6	27.7 ± 0.7	27.2 ± 0.6
APTT (%)	108.5 ± 5.3	109.6 ± 3.8	109.9 ± 4.6	113.0 ± 4.8	116.1 ± 4.3
Fibrinogen (mg/dl)	198.9 ± 14.8	203.8 ± 9.3	200.4 ± 10.2	193.6 ± 8.8	188.1 ± 12.1
Platelet surface marker					
PNC (%)	7.0 ± 0.8	6.4 ± 0.7	6.9 ± 0.7	6.6 ± 0.6	6.0 ± 0.8
PNC (ADP) (%)	17.8 ± 3.1	14.1 ± 2.0	15.5 ± 1.1	14.4 ± 2.5	15.9 ± 3.4
P-selectin (%)	12.9 ± 1.3	10.2 ± 0.4	11.3 ± 0.7	10.4 ± 0.7	10.5 ± 0.5
P-selectin (ADP) (%)	29.6 ± 2.7	26.6 ± 2.2	27.4 ± 2.4	26.2 ± 2.2	27.3 ± 2.2
Platelet maximal aggregation rate					
ADP (5 μmol/l) (%)	78 ± 3	67 ± 2**	66 ± 2**	65 ± 2**	66 ± 2**
ADP (1 μmol/l) (%)	31 ± 3	32 ± 4	33 ± 4	31 ± 4	33 ± 3
Collagen (2 μg/ml) (%)	85 ± 2	34 ± 6**	38 ± 6**	34 ± 5**	35 ± 6**
Collagen (0.25 μg/ml) (%)	23 ± 8	7 ± 2	8 ± 2	8 ± 1	7 ± 1
Endothelial function					
Diameter (before) (%)	0.367 ± 0.013	0.386 ± 0.014	0.375 ± 0.012	0.379 ± 0.013	0.379 ± 0.010
Heart rate (before) (bpm)	77 ± 10	76 ± 7	75 ± 8	72 ± 8	73 ± 7
Diameter (after) (%)	0.374 ± 0.013	0.396 ± 0.013	0.388 ± 0.013	0.391 ± 0.013	0.382 ± 0.009
Heart rate (after) (bpm)	77 ± 10	78 ± 9	73 ± 12	71 ± 8	73 ± 6
FMD ratio (%)	1.68 ± 0.29	2.78 ± 0.47	3.67 ± 0.41*	3.30 ± 0.50	1.07 ± 0.34$^{\#\$}$

Values are mean ± SE

RBC red blood cells, *WBC* white blood cells, *ADP* adenosine diphosphate, *PT* prothrombin time, *INR* international normalized ratio, *APTT* activated partial thromboplastin time, *PNC* platelet neutrophil complexes, *FMD* flow-mediated dilation

* $p < 0.05$ and ** $p < 0.01$ compared with baseline value (0 mg); $^{\#}$ $p < 0.01$ and $^{\$}$ $p < 0.01$ compared with values at 162 and 330 mg aspirin, respectively

effects (proportional reduction 13%). However, trials that examined doses of aspirin of ≥75 mg/day found a significant reduction in cardiovascular events, whereas three trials using doses of <75 mg/day did not. Similarly, a recent large trial of aspirin in primary prevention among women did not demonstrate a benefit of very-low-dose aspirin (100 mg every other day) [29]. No evidence supports the notion that daily aspirin doses of >1,000 mg is preferable for the prevention of serious vascular events among patients at high risk of stroke [7, 8]. One study found that the risk of the composite outcome of myocardial infarction, stroke or death within 3 months of carotid endarterectomy was significantly lower among patients taking 81 or 325 than 625–1,300 mg of aspirin daily [9]. In the present study, aspirin at doses above 81 mg suppressed platelet activity assessed by the aggregation test, P-selectin and PNC levels. This result is consistent with previous reports that show aspirin at even the low dose of 81 mg exerts antiplatelet effects.

Higher doses of aspirin can cause bleeding complication [7–9] and also impair endothelial function, which is known as the "aspirin dilemma" [10–12]. Aspirin inhibits a production of thromboxane A2 and cyclo-oxygenase enzyme, which synthesize thromboxane A2, a potent platelet aggregator in the platelets. Therefore, inhibiting thromboxane A2 is anti-thrombotic. Aspirin also inhibits cyclo-oxygenase enzyme in vascular endothelial cells, which is the source of prostaglandin I2, a vasodilator. A high dose of aspirin achieves both platelet inhibition

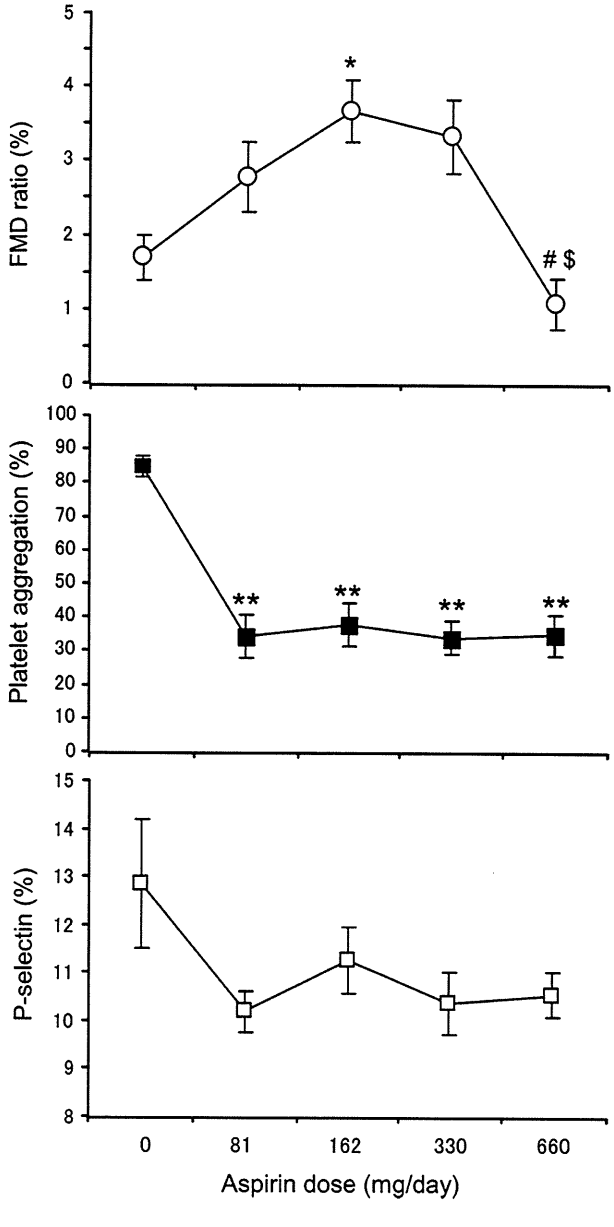

Fig. 1 FMD ratios (*upper panel*), maximal platelet aggregation rates (*middle panel*) and P-selectin levels (*lower panel*). Values are means ± SE. *FMD* Flow-mediated dilation. $^{*}p < 0.05$ from baseline (0 mg), $^{\#}p < 0.01$ from value at aspirin 162 mg, $^{\$}p < 0.01$ from value at 330 mg

and vasodilation, whereas a low dose spares endothelial cyclo-oxygenase activity and vasodilation. Therefore, the inhibition of prostaglandin I2 synthesis in the endothelial cells would increase the incidence of thromboembolic events. However, no clinical studies have examined endothelial function at various doses of aspirin, because endothelial function cannot be evaluated to determined platelet activity in a clinical setting. Endothelial function has recently been evaluated noninvasively as FMD to stratify patients according to cardiovascular risk, and endothelial dysfunction is associated with a poor prognosis [14–19]. Although a direct mechanism of decreased a FMD ratio at high dose of aspirin is uncertain, this could be due to high dose aspirin affecting vasodilation via endothelial cyclo-oxygenase inhibition.

Although FMD after reactive hyperemia is mainly mediated by NO synthesized in the endothelia [20, 21], another pathway associated with prostacyclin and thromboxane A2 mediates vascular reactivity [22–24]. Husain et al. [22] showed aspirin modulates acetylcholine-induced peripheral vasodilatation in patients with coronary atherosclerosis, and this effect may be due to the inhibition of vasoconstriction induced by one or more cyclo-oxygenases. Sun et al. [23] also showed that FMD is mediated by endothelium-derived prostanoids as it is blocked by indomethacin in eNOS knockout mice. Furthermore, Taubert et al. [24] showed a therapeutically relevant concentration of aspirin elicits NO release from the vascular endothelium independently of cyclo-oxygenase inhibition in in vitro study. These findings showed low dose aspirin could improve endothelial dysfunction and increase FMD. On the other hand, Gori et al. [30] reported 500 mg aspirin (once oral) did not affect the FMD ratio, but it significantly blunted low-flow-mediated constriction of the resting arterial tone. The difference from our results may be due to the dose and period of aspirin intake.

We found here that the FMD ratio increased at 162 mg from the baseline level without aspirin, and that this significantly decreased at a dose of 660 mg from that of 162 or 330 mg. Thus, low dose aspirin (<330 mg) did not deteriorate endothelial function, and 81 mg was sufficient to suppress platelet activity in healthy volunteers. However, platelets are more activated in patients with atherosclerosis than in normal individuals [31], and patients with atherosclerosis have endothelial dysfunction [14–19]. Moreover, several studies have indicated that patients at risk for atherosclerosis were less sensitive to the platelet inhibitory effect of aspirin [32–36]. Therefore, the optimal dose of aspirin might differ among patients with atherosclerosis compared with normal individuals, and aspirin doses of >81 mg might be required.

Platelet aggregation tests and FMD measurement might comprise an easy and noninvasive tool to determine the optimal dose of aspirin for such patients in a clinical setting. We applied the platelet aggregation test with light transmittance aggregometry and direct P-selectin measurements. Levels of platelet inhibition might be determined by evaluating several critical pathways [37]. That study used a new device based on light transmittance aggregometry that measures platelet activity more rapidly than classical devices and that could guide the choice of antiplatelet therapies. This method can evaluate patients

with aspirin resistance and optimize the dose, but cannot evaluate the extent to which various aspirin doses affect the endothelial function. On the other hand, FMD can evaluate the endothelial function affected by aspirin and generate useful information that could improve clinical outcomes.

Finally, the sample size in this study was small, and the subjects were normal male volunteers. Patients with atherosclerotic disease might have more activated platelets than normal individuals. Further studies are needed with a larger number of normal individuals and a cohort of patients with atherosclerotic disease.

Acknowledgments We thank Tadashi Ueta for excellent technical assistance. We also thank Misa Nakagawa, Yanan Zhang and Dongmei Zhang for technical assistance throughout the study.

References

1. Elwood PC, Cochrane AL, Burr ML, Sweetnam PM, Williams G, Welsby E, Hughes SJ, Renton R (1974) A randomized controlled trial of acetyl salicylic acid in the secondary prevention of mortality from myocardial infarction. Br Med J 1:436–440
2. Steering Committee of the Physicians' Health Study Research Group (1989) Final report on the aspirin component of the ongoing Physicians' Health Study. N Engl J Med 321:129–135
3. Peto R, Gray R, Collins R, Wheatley K, Hennekens C, Jamrozik K, Warlow C, Hafner B, Thompson E, Norton S, Gilliland J, Doll R (1988) Randomised trial of prophylactic daily aspirin in British male doctors. Br Med J (Clin Res Ed) 296(6618):313–316
4. Hebert PR, Hennekens CH (2000) An overview of the four randomized trials of aspirin therapy in the primary prevention of vascular disease. Arch Intern Med 160:3123–3127
5. Kubota N, Kasai T, Miyauchi K, Njaman W, Kajimoto K, Akimoto Y, Kojima T, Ken Y, Takeshi K, Hiroyuki D (2008) Therapy with statins and aspirin enhances long-term outcome of percutaneous coronary intervention. Heart Vessels 23:35–39
6. Antithrombotic Trialists' Collaboration (2002) Collaborative meta-analysis of randomised trials of antiplatelet therapy for prevention of death, myocardial infarction, and stroke in high risk patients. Br Med J 324:71–86
7. Dyken ML, Barnett HJ, Easton JD, Fields WS, Fuster V, Hachinski V, Norris JW, Sherman DG (1992) Low-dose aspirin and stroke. "It ain't necessarily so". Stroke 23:1395–1399
8. Barnett HJ, Kaste M, Meldrum H, Eliasziw M (1996) Aspirin dose in stroke prevention: beautiful hypotheses slain by ugly facts. Stroke 27:588–592
9. Taylor DW, Barnett HJ, Haynes RB, Ferguson GG, Sackett DL, Thorpe KE, Simard D, Silver FL, Hachinski V, Clagett GP, Barnes R, Spence JD (1999) Low-dose and high-dose acetylsalicylic acid for patients undergoing carotid endarterectomy: a randomised controlled trial. ASA and Carotid Endarterectomy (ACE) Trial Collaborators. Lancet 353:2179–2184
10. Moncada S, Gryglewski R, Bunting S, Vane JR (1976) An enzyme isolated from arteries transforms prostaglandin endoperoxides to an unstable substance that inhibits platelet aggregation. Nature 263:663–665
11. Willems C, De Groot PG, Pool GA, Gonsalvez MS, Van Aken WG, Van Mourik JA (1982) Arachidonate metabolism in cultured human vascular endothelial cells. Evidence for two prostaglandin synthetic pathways sensitive to acetylsalicylic acid. Biochim Biophys Acta 713:581–588
12. Ozturk O, Greaves M, Templeton A (2002) Aspirin dilemma. Remodelling the hypothesis from a fertility perspective. Hum Reprod 17:1146–1148
13. Corretti MC, Anderson TJ, Benjamin EJ, Celermajer D, Charbonneau F, Creager MA, Deanfield J, Drexler H, Gerhard-Herman M, Herrington D, Vallance P, Vita J, Vogel R, International Brachial Artery Reactivity Task Force (2002) Guidelines for the ultrasound assessment of endothelial-dependent flow-mediated vasodilation of the brachial artery: a report of the International Brachial Artery Reactivity Task Force. J Am Coll Cardiol 39:257–265
14. Witte DR, Westerink J, de Koning EJ, van der Graaf Y, Grobbee DE, Bots ML (2005) Is the association between flow-mediated dilation and cardiovascular risk limited to low-risk populations? J Am Coll Cardiol 45:1987–1993
15. Dogra G, Rich L, Stanton K, Watts GF (2001) Endothelium-dependent and independent vasodilation studies at normoglycaemia in type I diabetes mellitus with and without microalbuminuria. Diabetologia 44:593–601
16. Yeboah J, Crouse JR, Hsu FC, Burke GL, Herrington DM (2007) Brachial flow-mediated dilation predicts incident cardiovascular events in older adults: the Cardiovascular Health Study. Circulation 115:2390–2397
17. Mizia-Stec K, Gasior Z, Zahorska-Markiewicz B, Holecki M, Haberka M, Mizia M, Gomułka S, Zak-Gołab A, Gościńska A (2008) The indexes of arterial structure and function in women with simple obesity: a preliminary study. Heart Vessels 23:224–229
18. Fujii N, Tsuchihashi K, Sasao H, Eguchi M, Miurakami H, Hase M, Higashiura K, Yuda S, Hashimoto A, Miura T, Ura N, Shimamoto K (2008) Insulin resistance functionally limits endothelium-dependent coronary vasodilation in nondiabetic patients. Heart Vessels 23:9–15
19. Crisby M, Kublickiene K, Henareh L, Agewall S (2009) Circulating levels of autoantibodies to oxidized low-density lipoprotein and C-reactive protein levels correlate with endothelial function in resistance arteries in men with coronary heart disease. Heart Vessels 24:90–95
20. Pohl U, Holtz J, Busse R, Bassenge E (1986) Crucial role of endothelium in the vasodilator response to increased flow in vivo. Hypertension 8:37–44
21. Joannides R, Haefeli WE, Linder L, Richard V, Bakkali EH, Thuillez C, Lüscher TF (1995) Nitric oxide is responsible for flow-dependent dilatation of human peripheral conduit arteries in vivo. Circulation 91:1314–1319
22. Husain S, Andrews NP, Mulcahy D, Panza JA, Quyyumi AA (1998) Aspirin improves endothelial dysfunction in atherosclerosis. Circulation 97:716–720
23. Sun D, Huang A, Smith CJ, Stackpole CJ, Connetta JA, Shesely EG, Koller A, Kaley G (1999) Enhanced release of prostaglandins contributes to flow-induced arteriolar dilation in eNOS knockout mice. Circ Res 85:288–293
24. Taubert D, Berkels R, Grosser N, Schröder H, Gründemann D, Schömig E (2004) Aspirin induces nitric oxide release from vascular endothelium: a novel mechanism of action. Br J Pharmacol 143:159–165
25. Born GV (1962) Aggregation of blood platelets by adenosine diphosphate and its reversal. Nature 194:927–929
26. O'brien JR (1962) Platelet aggregation: Part I some effects of the adenosine phosphates, thrombin, and cocaine upon platelet adhesiveness. J Clin Pathol 15:446–452
27. Peters MJ, Heyderman RS, Hatch DJ, Klein NJ (1997) Investigation of platelet-neutrophil interactions in whole blood by flow cytometry. J Immunol Methods 209:125–135
28. Yamasaki F, Furuno T, Sato K, Zhang D, Nishinaga M, Sato T, Doi Y, Sugiura T (2005) Association between arterial stiffness and platelet activation. J Hum Hypertens 19:527–533